

**Figure 3.** The *Hsp90 $\alpha$*  KO mutation reduced L1-derived piRNAs, but not piRNA-related 16- or 19-nt small RNAs. (A) The length distributions of small RNAs in the WT (black) and *Hsp90 $\alpha$*  KO (red) libraries that were mapped to the consensus sequence of the A-type L1 retrotransposon. The sense (top) and antisense (bottom) RNAs are separately presented. (B) Length distribution of distances between the 5'-end of 24–33-nt small RNAs mapped to the sense strand of the L1 sequence and the 5'-end of 24–33-nt small RNAs mapped to the L1 antisense strand. Blue line, WT library; red line, KO library. (C) Configuration of 16- and 19-nt small RNAs derived from the L1 sequence. For many 16- and 19-nt small RNAs, their end positions are 1 bp upstream of the start position of 24–33-nt small RNAs on the same strand, and their start positions are the same position as the end position of 26- and 29-nt small RNAs on the opposite strand. The two piRNA-length small RNAs overlap each other by 10 bp. See also Supplementary Figure S2 for details. (D) The length distributions of small RNAs in the WT (blue) and *Hsp90 $\alpha$*  KO (red) libraries that were mapped to the previously identified piRNA clusters.

ure 3D). Therefore, these 19-nt RNAs are likely the byproducts of piRNA production via the ping-pong cycle, as has been suggested for 19-nt RNAs present in adult testes containing pachytene and prepachytene piRNAs (38,39). In addition, the presence of 16-nt byproducts was evident (Figure 3A, C and Supplementary Figure S2). The amounts of these 19- and 16-nt byproducts were only slightly reduced by the *Hsp90 $\alpha$*  mutation. It has been reported that in cultured silkworm cells, chemical inhibition of HSP90 results in the accumulation of such 16-nt byproducts in the PIWI complex, suggesting that HSP90 facilitates the recycling of PIWI for efficient ping-pong cycling (15). In the mouse system, however, our data imply that neither RNA cleavage nor PIWI recycling is affected by HSP90 $\alpha$  inactivation; thus, it appears more likely that HSP90 $\alpha$  plays a role in stabilizing 24–33-nt piRNAs, such as stabilizing piRNA–protein complexes.

### L1 retrotransposons are derepressed in the fetal germ cells of *Hsp90 $\alpha$* KO mice

The reduction of L1-derived 24–33-nt piRNAs prompted us to investigate whether the expression of this retrotransposon is misregulated in mutant prospermatogonia. Thus, we compared the expression of the L1-encoded ORF1p protein in WT and *Hsp90 $\alpha$*  KO testes at E18.5 by immunofluorescence. The number of ORF1p-positive germ cells was significantly increased in the fetal *Hsp90 $\alpha$*  KO testis (Figure 4A). Furthermore, western blotting of the whole testes lysates (E16.5) revealed a definite increase in ORF1p levels in the mutant testes (Figure 4B). In contrast, L1 mRNA levels were largely unchanged in these testes (Figure 4C), suggesting that the effect occurs at the post-transcriptional level. Consistently, the DNA methylation levels of the promoter sequences of A- and Gf-type L1 were largely similar between WT and KO P0 prospermatogonia (Figure 4D).

### Postnatal piRNA levels derived from retrotransposons were reduced in *Hsp90 $\alpha$* KO mice

We also investigated the effect of the *Hsp90 $\alpha$*  KO mutation on piRNA biogenesis and DNA methylation in postnatal germ cells. Northern blot analysis of testis RNA on postnatal day 24 (P24) against piRNA derived from IAP, another active retrotransposon, revealed a severe reduction in piRNA levels in the mutant testes (Figure 5A). The reduction of L1-derived piRNA was unclear because of smearing; however, longer RNAs were accumulated in the mutant testes, very similarly to *Mitopl*d KO testes, which are deficient in piRNA production and show an increased L1 mRNA level at postnatal stages (18). These results suggest that, at the postnatal stages, L1 transcription is increased in *Hsp90 $\alpha$*  KO testes. The DNA methylation level in the L1 promoters was partially reduced in the *Hsp90 $\alpha$*  mutant testes at P15 when analyzed by methylation-sensitive enzyme digestion and Southern blot, although it was not as much as *Mitopl*d KO testes (Figure 5B). However, when analyzed by bisulfite sequencing, the L1 promoters were normally methylated in *Hsp90 $\alpha$*  KO meiotic germ cells (spermatocytes) at P17 (Figure 5C), as in the P0 prospermatogonia (Figure 4D). Although there might be a difference in

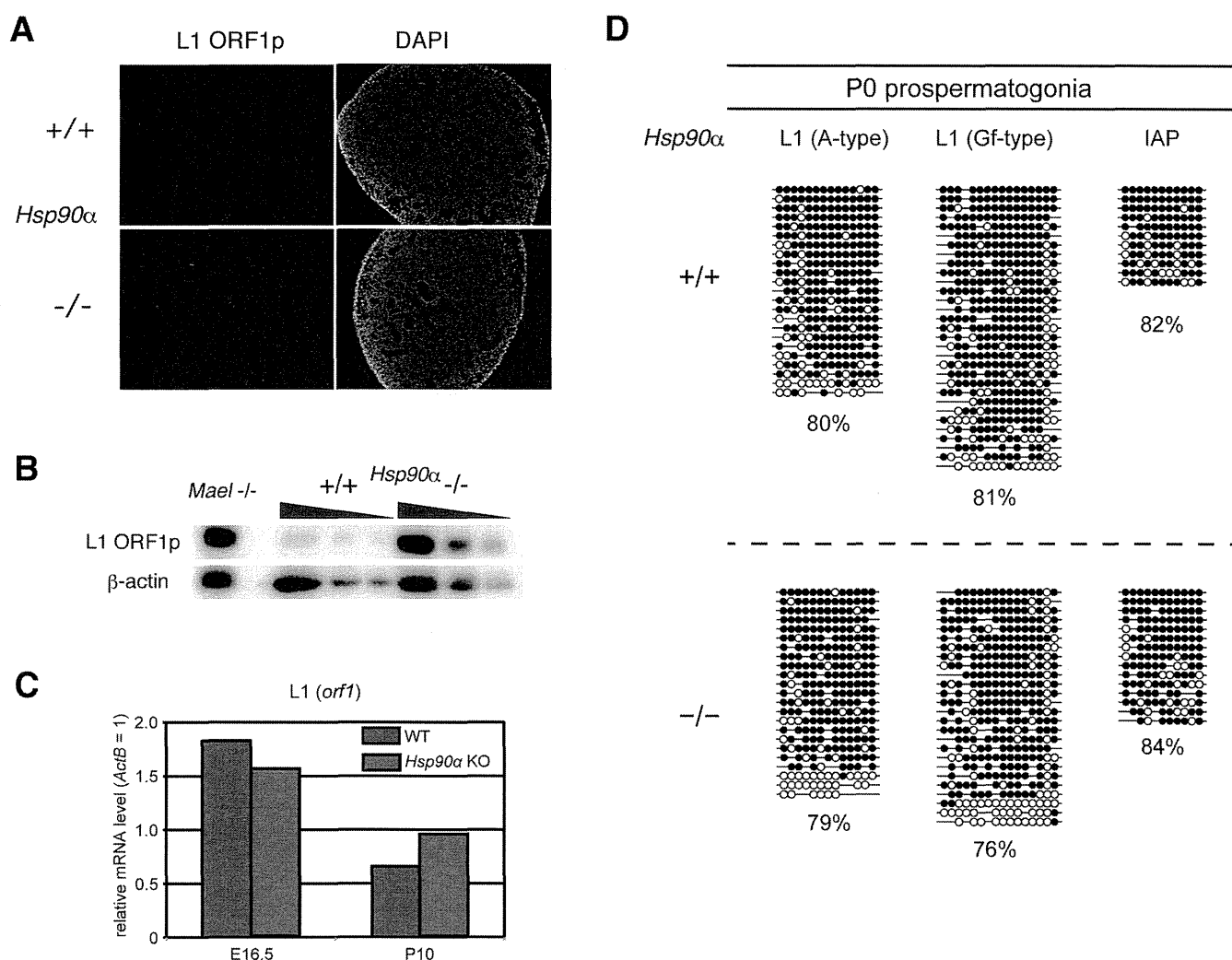


**Figure 4.** Increase in L1-encoded protein levels in *Hsp90α* KO testes. (A) Immunofluorescence detection of L1 ORF1 protein in E18.5 testes. (B) Western blot analysis of L1 ORF1 protein in E16.5 testes lysates. *Maelstrom* KO testis lysate (gifted from Dr A. Bortvin) was used as a positive control, and  $\beta$ -actin served as a loading control. (C) The gene expression of L1 *orf1* in WT (blue) and *Hsp90α* KO (red) testes at E16.5 and P10 was determined by quantitative RT-PCR and normalized by the *ActB* expression level. (D) DNA methylation levels of retrotransposon sequences in WT and KO prospermatogonia (at P0) determined by bisulfite-PCR sequencing. Open and closed circles represent unmethylated and methylated CpG sites, respectively.

methylation in several limited loci of L1, the profound decrease in piRNA production did not affect DNA methylation of a bulk of L1 promoters.

## DISCUSSION

The HSP90 proteins play a pivotal role for maintaining the integrity of cellular functions by supporting the activities of many client proteins, and this HSP90's function has been proposed to be important for the robustness of developmental pathways under genetic or environmental perturbations (i.e. canalization) (40,41). In the germ cells, maintaining the integrity of the genome and epigenome is especially important, because they convey the genetic and possibly epigenetic information to the progenies. The germline piRNA system is an efficient host defense system against the mutagenic effects of active transposons by cleaving their RNAs and epigenetically silencing their promoters. We recently revealed that *Hsp90α* is essential for spermatogen-

esis (17), and in this report, we showed that HSP90 $\alpha$  is important for piRNA production and post-transcriptional repression of retrotransposons in mouse fetal germ cells. Several proteins indispensable for piRNA production have been identified, and there are even more proteins regulating these key proteins. The PIWI-clade Argonaute proteins, MILI and MIWI2, are the most centered in the mouse fetal piRNA system as they form complexes with primary piRNAs, cleave the transposon-derived RNAs to generate secondary piRNAs and mediate DNA methylation of transposons such as L1. The loss of HSP90 $\alpha$  decreased both MILI- and MIWI2-bound fractions of fetal piRNAs by ~3-fold, but not completely. The remaining piRNAs showed the hallmarks of ping-pong cycle, which indicate that the RNase (slicer) activity of the PIWI protein(s) is still working in KO germ cells. Nevertheless, the decrease was enough to derepress retrotransposons.

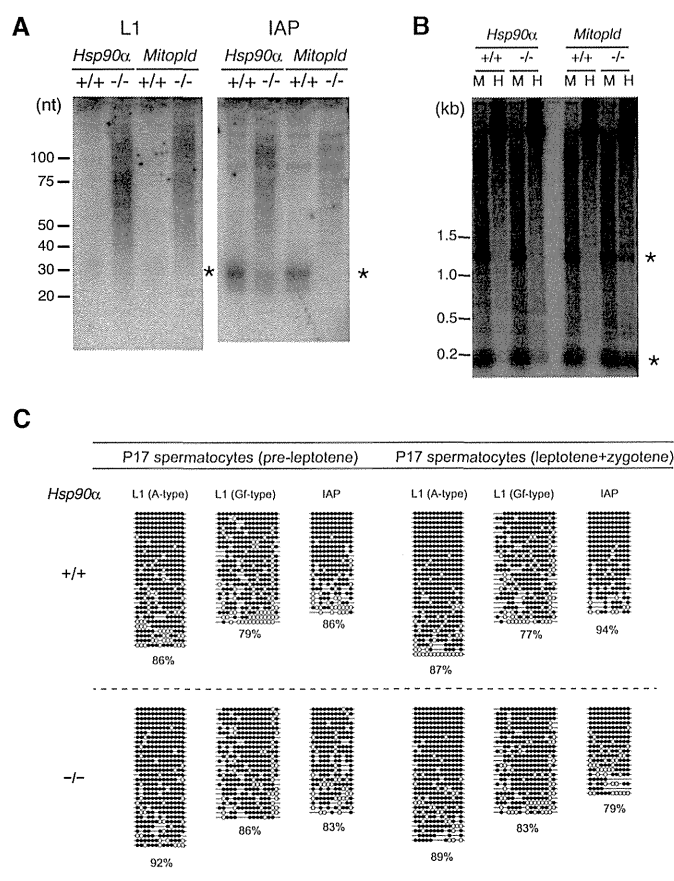


**Figure 5.** The expression levels of piRNA and the DNA methylation of L1 and IAP retrotransposons. (A) Northern blot analysis of piRNAs derived from L1 and IAP in P24 testes. *Mitoplδ* KO testes were used as a control for piRNA defects. (B) DNA methylation state of L1 5'-UTR was detected by Southern blot analysis of testes DNA digested by a methylation-insensitive (*Msp*I; M) or methylation-sensitive (*Hpa*II; H) restriction enzyme. (A, B) Asterisks indicate the expected band sizes. (C) DNA methylation levels of retrotransposon sequences in WT and KO spermatocytes (at P17) determined by bisulfite-PCR sequencing. Open and closed circles represent unmethylated and methylated CpG sites, respectively.

The reports on the piRNA system have been accumulating in this decade. However, the mechanisms of piRNA-mediated retrotransposon silencing are still not fully understood, especially in the series of steps: (i) the loading of MILI-generated piRNAs onto MIWI2, (ii) the translocation of MIWI2-piRNA complex into nucleus and (iii) the introduction of DNA methylation in retrotransposon promoters. TDRD9, which contains a Tudor domain recognizing methylated arginine residues, has been shown to co-localize with and binds to MIWI2 at piP-bodies and both proteins are also present in nucleus, suggesting its role in the MIWI2 translocation (25). The other PIWI proteins in postnatal germ cells, MILI and MIWI, have been shown to be methylated by an HSP90 client protein, PRMT5, which is a type II protein methyltransferase (32,33). However, it was unknown whether MIWI2 is methylated *in vivo*, although MIWI2 has the PRMT5-methylation motif and can be methylated by PRMT5 *in vitro* (32,33). Here, we showed that MIWI2 is indeed methylated in fetal germ cells. But, it is likely that the level of the MIWI2 methylation was not

affected in prospermatogonia at E16.5 by the *Hsp90α* deficiency, demonstrating that the arginine methylation is not sufficient for the MIWI2 protein to translocate into nuclei. Interestingly, even with the arginine methylation of MIWI2, the subcellular localization patterns of MIWI2 and TDRD9 became different in *Hsp90α* KO germ cells; TDRD9 still can enter the nucleus in the mutant. Given the function of HSP90α in protein transport across membranes in dendritic cells (16,24), it is tempting to speculate that HSP90α may function as a chaperone for MIWI2 translocation. This prospect should be explored in future studies.

Despite the low efficiency of MIWI2 nuclear translocation and the low amount of piRNAs, the DNA methylation levels at L1 promoters were not severely affected. Therefore, the small amounts of MIWI2-piRNA complexes in the nucleus might be enough to guide *de novo* DNA methylation of the retrotransposon promoters. We showed that L1 mRNA is highly produced even in the WT fetal testes and is not extra-elevated in the *Hsp90α* KO testes. On the other hand, the amount of the L1-encoded protein was significantly elevated in the *Hsp90α* mutant testes. These features, i.e. *de novo* DNA methylation is not affected but the expression of L1 is elevated at the protein level, are very similar to the phenotype of the mutant of *Maelstrom* (28), a gene known to be involved in the piRNA-based transposon silencing system. Therefore, L1 is repressed at the post-transcriptional level in fetal male germ cells (prospermatogonia), and *Maelstrom* and HSP90α are likely involved in it. On the other hand, the piRNA-guided DNA methylation at the L1 promoter is important for transcriptional silencing in later (postnatal) stages, as evidenced by an increase in L1 mRNA after birth in the *Mili* and *Miwi2* mutants (23,42-43). HSP90α is possibly involved in several distinct steps in normal male germ cell development, because HSP90 is a chaperone that stabilizes a numerous client proteins in cytosol and in nucleus. Further study is needed to elucidate whether the deficiency in post-transcriptional regulation of retrotransposons in the *Hsp90α* KO fetal germ cells is directly linked to the deficiency in piRNA biogenesis.

Involvement of the HSP90 chaperone complexes in the mouse piRNA biogenesis was first suggested in the study of FKBP6, HSP90's co-chaperone, in which the authors showed that the *Fkbp6* KO mice had a defect in piRNA production, especially in MIWI2-bound piRNA (15). They also analyzed the effect of an HSP90 inhibitor, Geldanamycin (GA), on the piRNA biogenesis in cultured silkworm cells. The GA-treatment resulted in the accumulation of additional ~16-bp small RNA species which are likely byproducts of the RNA cleavage reaction by Ago3, a PIWI protein. Thus, they suggested that FKBP6 in mice and HSP90 in silkworm are involved in efficient recycling of the slicer enzyme. On the other hand, our computational analysis on the published sequence data revealed that the ping-pong byproducts are not accumulated in *Fkbp6* KO testes, similarly to the *HSP90α* KO testes. It is of note that, in *Hsp90α* KO testes, not only MIWI2-bound piRNAs but also MILI-bound piRNAs are reduced, indicating the presence of both FKBP6-dependent and FKBP6-independent actions of HSP90α. This seems to parallel with the insect piRNA system where at least two different HSP90 co-chaperones, Hop and Shutdown (*Fkbp6* ortholog), are

required (12,14). The reduction of both MILI- and MIWI2-bound piRNAs by the *Hsp90α* mutation also suggests that the steps where HSP90α is involved in the piRNA biogenesis pathway include a step(s) upstream of the enzymatic reactions by MILI. Therefore, in analogy to the role of the insect HSP90 machinery in the formation of piRNA-PIWI complex (13) and siRNA-Ago2 complex (8), it is conceivable that the mouse HSP90α machinery has important roles in the formation and/or stability of the MILI-piRNA and MIWI2-piRNA complexes, the later being dependent on the FKBP6 co-chaperone.

The two cytosolic HSP90 isoforms were generated by gene duplication in the common ancestor of vertebrates and maintained thereafter, with the amino acid sequence and the expression pattern being diverged (44). However, whether the two isoforms are *functionally* diverged, particularly whether HSP90α with more tissue-specific expression has indispensable functions, remains controversial. A function specific to HSP90α would be its extracellular role in regulating matrix metalloproteinase activity and cancer metastasis (45). However, little is known about the difference in their intracellular functions. We previously demonstrated that HSP90α plays a more important role than HSP90β in the membrane translocation and presentation of exogenous antigens in mouse dendritic cells (16,24). In this study, our data revealed that HSP90α plays specific roles in the epigenetic regulatory systems against transposons during germ cell development. The single insect gene of HSP90 is also involved in piRNA biogenesis and transposon silencing (11,12), hinting that the function of the HSP90 machinery in piRNA biogenesis is conserved in metazoans. After gene duplication and functional divergence, this piRNA-related function may have become specific to *Hsp90α* in vertebrates or at least in mammals. Then, under the selection, *Hsp90α* may have become highly expressed in male germ cells.

## ACCESSION NUMBERS

The small RNA sequencing data were deposited in GEO under the accession no. GSE54515.

## SUPPLEMENTARY DATA

Supplementary Data are available at NAR Online.

## ACKNOWLEDGEMENT

We thank Dr Alex Bortvin (Carnegie Institute) for supplying the anti-L1 antibody and Drs Takehisa Sakaguchi and Takashi Sado (Kyushu University) for technical advice. Ms Megumi Iwata is acknowledged for her technical assistance. We also thank Dr Akihiro Matsukawa and Mr Haruyuki Watanabe (Okayama University) for the use of the cryostat.

## FUNDING

Grants-in-aid for Scientific Research from the Ministry of Education, Culture, Sports, Science, and Technology of Japan [22501027 to H.U., 20062010 to H.S., 25503003 and 21200037 to K.I.]; Takeda Foundation (to K.I. and H.U.);

Naito Foundation (to H.U.); Women Researchers' Hand-in-Hand Program at Kyushu University (to T.I.). Funding for open access charge: The Takeda Foundation (to H.U.). *Conflict of interest statement.* None declared.

## REFERENCES

1. Taipale, M., Jarosz, D.F. and Lindquist, S. (2010). HSP90 at the hub of protein homeostasis: emerging mechanistic insights. *Nat. Rev. Mol. Cell Biol.*, **11**, 515–528.
2. Wandinger, S.K., Richter, K. and Buchner, J. (2008). The Hsp90 chaperone machinery. *J. Biol. Chem.*, **283**, 18473–18477.
3. Ohsako, S., Bunick, D. and Hayashi, Y. (1995). Immunocytochemical observation of the 90 KD heat shock protein (HSP90): high expression in primordial and pre-meiotic germ cells of male and female rat gonads. *J. Histochem. Cytochem.*, **43**, 67–76.
4. Lee, S.J. (1990). Expression of HSP86 in male germ cells. *Mol. Cell Biol.*, **10**, 3239–3242.
5. Vanmuylder, N., Werry-Huet, A., Rooze, M. and Louryan, S. (2002). Heat shock protein HSP86 expression during mouse embryo development, especially in the germ-line. *Anat. Embryol.*, **205**, 301–306.
6. Iki, T., Yoshikawa, M., Nishikiori, M., Jaudal, M.C., Matsumoto-Yokoyama, E., Mitsuhashi, I., Meshi, T. and Ishikawa, M. (2010). In vitro assembly of plant RNA-induced silencing complexes facilitated by molecular chaperone HSP90. *Mol. Cell*, **39**, 282–291.
7. Iwasaki, S., Kobayashi, M., Yoda, M., Sakaguchi, Y., Katsuma, S., Suzuki, T. and Tomari, Y. (2010). Hsc70/Hsp90 chaperone machinery mediates ATP-dependent RISC loading of small RNA duplexes. *Mol. Cell*, **39**, 292–299.
8. Miyoshi, T., Takeuchi, A., Siomi, H. and Siomi, M.C. (2010). A direct role for Hsp90 in pre-RISC formation in *Drosophila*. *Nat. Struct. Mol. Biol.*, **17**, 1024–1026.
9. Pare, J.M., Tahbaz, N., Lopez-Orozco, J., LaPointe, P., Lasko, P. and Hobman, T.C. (2009). Hsp90 regulates the function of argonaute 2 and its recruitment to stress granules and P-bodies. *Mol. Biol. Cell*, **20**, 3273–3284.
10. Pillai, R.S. and Chuma, S. (2012). piRNAs and their involvement in male germline development in mice. *Dev. Growth Differ.*, **54**, 78–92.
11. Specchia, V., Piacentini, L., Tritto, P., Fanti, L., D'Alessandro, R., Palumbo, G., Pimpinelli, S. and Bozzetti, M.P. (2010). Hsp90 prevents phenotypic variation by suppressing the mutagenic activity of transposons. *Nature*, **463**, 662–665.
12. Gangaraju, V.K., Yin, H., Weiner, M.M., Wang, J., Huang, X.A. and Lin, H. (2011). *Drosophila* Piwi functions in Hsp90-mediated suppression of phenotypic variation. *Nat. Genet.*, **43**, 153–158.
13. Izumi, N., Kawaoka, S., Yasuhara, S., Suzuki, Y., Sugano, S., Katsuma, S. and Tomari, Y. (2013). Hsp90 facilitates accurate loading of precursor piRNAs into PIWI proteins. *RNA*, **19**, 896–901.
14. Olivieri, D., Senti, K.A., Subramanian, S., Sachidanandam, R. and Brennecke, J. (2012). The cochaperone shutdown defines a group of biogenesis factors essential for all piRNA populations in *Drosophila*. *Mol. Cell*, **47**, 954–969.
15. Xiol, J., Cora, E., Koglgruber, R., Chuma, S., Subramanian, S., Hosokawa, M., Reuter, M., Yang, Z., Berninger, P., Palencia, A. *et al.* (2012). A role for Fkbp6 and the chaperone machinery in piRNA amplification and transposon silencing. *Mol. Cell*, **47**, 970–979.
16. Imai, T., Kato, Y., Kajiwara, C., Mizukami, S., Ishige, I., Ichianagi, T., Hikida, M., Wang, J.Y. and Udono, H. (2011). Heat shock protein 90 (HSP90) contributes to cytosolic translocation of extracellular antigen for cross-presentation by dendritic cells. *Proc. Natl. Acad. Sci. U.S.A.*, **108**, 16363–16368.
17. Kajiwara, C., Kondo, S., Uda, S., Dai, L., Ichianagi, T., Chiba, T., Ishido, S., Koji, T. and Udono, H. (2012). Spermatogenesis arrest caused by conditional deletion of Hsp90alpha in adult mice. *Biol. Open*, **1**, 977–982.
18. Watanabe, T., Chuma, S., Yamamoto, Y., Kuramochi-Miyagawa, S., Totoki, Y., Toyoda, A., Hoki, Y., Fujiyama, A., Shibata, T., Sado, T. *et al.* (2011). MITOPLD is a mitochondrial protein essential for nuage formation and piRNA biogenesis in the mouse germline. *Dev. Cell*, **20**, 364–375.

19. Martin, S.L. and Branciforte, D. (1993). Synchronous expression of LINE-1 RNA and protein in mouse embryonal carcinoma cells. *Mol. Cell. Biol.*, **13**, 5383–5392.
20. Kozomara, A. and Griffiths-Jones, S. (2014). miRBase: annotating high confidence microRNAs using deep sequencing data. *Nucleic Acids Res.*, **42**, D68–D73.
21. Jiang, H. and Wong, W.H. (2008). SeqMap: mapping massive amount of oligonucleotides to the genome. *Bioinformatics*, **24**, 2395–2396.
22. Jurka, J., Kapitonov, V.V., Pavlicek, A., Klonowski, P., Kohany, O. and Walichiewicz, J. (2005). Repbase Update, a database of eukaryotic repetitive elements. *Cytogen. Genome Res.*, **110**, 462–467.
23. Kuramochi-Miyagawa, S., Watanabe, T., Gotoh, K., Totoki, Y., Toyoda, A., Ikawa, M., Asada, N., Kojima, K., Yamaguchi, Y., Ijiri, T.W. *et al.* (2008). DNA methylation of retrotransposon genes is regulated by Piwi family members MIL1 and MIWI2 in murine fetal testes. *Genes Dev.*, **22**, 908–917.
24. Ichianagi, T., Imai, T., Kajiwara, C., Mizukami, S., Nakai, A., Nakayama, T. and Udono, H. (2010). Essential role of endogenous heat shock protein 90 of dendritic cells in antigen cross-presentation. *J. Immunol.*, **185**, 2693–2700.
25. Shoji, M., Tanaka, T., Hosokawa, M., Reuter, M., Stark, A., Kato, Y., Kondoh, G., Okawa, K., Chujo, T., Suzuki, T. *et al.* (2009). The TDRD9-MIWI2 complex is essential for piRNA-mediated retrotransposon silencing in the mouse male germline. *Dev. Cell*, **17**, 775–787.
26. Bastos, H., Lassalle, B., Chicheportiche, A., Riou, L., Testart, J., Allemand, I. and Fouchet, P. (2005). Flow cytometric characterization of viable meiotic and postmeiotic cells by Hoechst 33342 in mouse spermatogenesis. *Cytometry A*, **65**, 40–49.
27. Ichianagi, K., Li, Y., Watanabe, T., Ichianagi, T., Fukuda, K., Kitayama, J., Yamamoto, Y., Kuramochi-Miyagawa, S., Nakano, T., Yabuta, Y. *et al.* (2011). Locus- and domain-dependent control of DNA methylation at mouse B1 retrotransposons during male germ cell development. *Genome Res.*, **21**, 2058–2066.
28. Aravin, A.A., van der Heijden, G.W., Castaneda, J., Vagin, V.V., Hannon, G.J. and Bortvin, A. (2009). Cytoplasmic compartmentalization of the fetal piRNA pathway in mice. *PLoS Genet.*, **5**, e1000764.
29. Olovnikov, I., Aravin, A.A. and Fejes Toth, K. (2012). Small RNA in the nucleus: the RNA-chromatin ping-pong. *Curr. Opin. Genet. Dev.*, **22**, 164–171.
30. Wang, J., Saxe, J.P., Tanaka, T., Chuma, S. and Lin, H. (2009). Mili interacts with tudor domain-containing protein 1 in regulating spermatogenesis. *Curr. Biol.*, **19**, 640–644.
31. Chen, C., Nott, T.J., Jin, J. and Pawson, T. (2011). Deciphering arginine methylation: Tudor tells the tale. *Nat. Rev. Mol. Cell Biol.*, **12**, 629–642.
32. Vagin, V.V., Wohlschlegel, J., Qu, J., Jonsson, Z., Huang, X., Chuma, S., Girard, A., Sachidanandam, R., Hannon, G.J. and Aravin, A.A. (2009). Proteomic analysis of murine Piwi proteins reveals a role for arginine methylation in specifying interaction with Tudor family members. *Genes Dev.*, **23**, 1749–1762.
33. Saxe, J.P., Chen, M., Zhao, H. and Lin, H. (2013). Tdrkh is essential for spermatogenesis and participates in primary piRNA biogenesis in the germline. *EMBO J.*, **3**, 1869–1885.
34. Maloney, A., Clarke, P.A., Naaby-Hansen, S., Stein, R., Koopman, J.O., Akpan, A., Yang, A., Zvelebil, M., Cramer, R., Stimson, L. *et al.* (2007). Gene and protein expression profiling of human ovarian cancer cells treated with the heat shock protein 90 inhibitor 17-allylamino-17-demethoxygeldanamycin. *Cancer Res.*, **67**, 3239–3253.
35. Aravin, A.A., Sachidanandam, R., Bourc'his, D., Schaefer, C., Pezic, D., Toth, K.F., Bestor, T. and Hannon, G.J. (2008). A piRNA pathway primed by individual transposons is linked to de novo DNA methylation in mice. *Mol. Cell*, **31**, 785–799.
36. Soper, S.F., van der Heijden, G.W., Hardiman, T.C., Goodheart, M., Martin, S.L., de Boer, P. and Bortvin, A. (2008). Mouse maelstrom, a component of nuage, is essential for spermatogenesis and transposon repression in meiosis. *Dev. Cell*, **15**, 285–297.
37. Zheng, K., Xiol, J., Reuter, M., Eckardt, S., Leu, N.A., McLaughlin, K.J., Stark, A., Sachidanandam, R., Pillai, R.S. and Wang, P.J. (2010). Mouse MOV10L1 associates with Piwi proteins and is an essential component of the Piwi-interacting RNA (piRNA) pathway. *Proc. Natl. Acad. Sci. U.S.A.*, **107**, 11841–11846.
38. Oey, H.M., Youngson, N.A. and Whitelaw, E. (2011). The characterisation of piRNA-related 19mers in the mouse. *BMC Genomics*, **12**, 315.
39. Berninger, P., Jaskiewicz, L., Khorshid, M. and Zavolan, M. (2011). Conserved generation of short products at piRNA loci. *BMC Genomics*, **12**, 46.
40. Rutherford, S.L. and Lindquist, S. (1998). Hsp90 as a capacitor for morphological evolution. *Nature*, **396**, 336–342.
41. McLaren, A. (1999). Too late for the midwife toad: stress, variability and Hsp90. *Trends Genet.*, **15**, 169–171.
42. Carmell, M.A., Girard, A., de Kant, H.J., Bourc'his, D., Bestor, T.H., de Rooij, D.G. and Hannon, G.J. (2007). MIWI2 is essential for spermatogenesis and repression of transposons in the mouse male germline. *Dev. Cell*, **12**, 503–514.
43. Aravin, A.A., Sachidanandam, R., Girard, A., Fejes-Toth, K. and Hannon, G.J. (2007). Developmentally regulated piRNA clusters implicate MIL1 in transposon control. *Science*, **316**, 744–747.
44. Chen, B., Zhong, D. and Monteiro, A. (2006). Comparative genomics and evolution of the HSP90 family of genes across all kingdoms of organisms. *BMC Genomics*, **7**, 156.
45. Eustace, B.K., Sakurai, T., Stewart, J.K., Yimlamai, D., Unger, C., Zehetmeier, C., Lain, B., Torella, C., Henning, S.W., Beste, G. *et al.* (2004). Functional proteomic screens reveal an essential extracellular role for hsp90 alpha in cancer cell invasiveness. *Nat. Cell Biol.*, **6**, 507–514.

We have shown that transcriptional noise is well predicted by molecularly detailed models for the two most common promoter architectures in *E. coli* as the various genetic knobs are tuned. This agreement is not the result of fitting theory curves to data, because the predicted curves are generated using physical parameter values reported elsewhere in the literature and in that sense are zero-parameter predictions. Earlier reports of “bursty” transcription (5, 21) are based on the observation that the Fano factor is greater than 1 for constitutive mRNA production (as well as direct kinetic measurements). Various explanatory hypotheses have been proposed, including transcriptional silencing via DNA condensation by nucleoid proteins (22), negative supercoiling induced by transcription, or the formation of long-lived “dead-end” initiation complexes (23). Although our data do not rule out these hypotheses, we find that extrinsic noise is sufficient to explain the deviation from Fano = 1 in our constitutive expression data (Fig. 2B). Thus, we find no need to invoke alternative hypotheses to explain the observed “burstiness” of constitutive transcription.

Many interesting earlier experiments make it difficult to interpret differences between promoters and induction conditions in terms of distinct physical parameters because of the wide variety of promoter architectures in play as well as the diverse mechanisms of induction. We have instead taken a “synthetic biology” approach of building promoters from the ground up. By directly controlling aspects of the promoter architecture, our goal has been to directly relate changes in promoter architecture to changes in observed gene expression variability. We believe that this work has demonstrated that mutations in regulatory DNA can alter gene expression noise. This suggests that gene expression noise may be a tunable property subject to evolutionary selection pressure, as mutations in regulatory DNA could provide greater fitness by increasing (or decreasing) variability. Demonstrating the relevance of this hypothesis in natural environments remains an ongoing challenge.

## REFERENCES AND NOTES

1. J. Paulsson, M. Ehrenberg, *Phys. Rev. Lett.* **84**, 5447–5450 (2000).
2. A. Sanchez, H. G. Garcia, D. Jones, R. Phillips, J. Kondev, *PLoS Comput. Biol.* **7**, e1001100 (2011).
3. Y. Taniguchi *et al.*, *Science* **329**, 533–538 (2010).
4. W. J. Blake *et al.*, *Mol. Cell* **24**, 853–865 (2006).
5. L. H. So *et al.*, *Nat. Genet.* **43**, 554–560 (2011).
6. H. Salman *et al.*, *Phys. Rev. Lett.* **108**, 238105 (2012).
7. H. Maamar, A. Raj, D. Dubnau, *Science* **317**, 526–529 (2007).
8. A. Eldar, M. B. Elowitz, *Nature* **467**, 167–173 (2010).
9. G. M. Suel, R. P. Kulkarni, J. Dworkin, J. Garcia-Ojalvo, M. B. Elowitz, *Science* **315**, 1716–1719 (2007).
10. M. Thattai, A. van Oudenaarden, *Genetics* **167**, 523–530 (2004).
11. E. Kussell, S. Leibler, *Science* **309**, 2075–2078 (2005).
12. H. Salgado *et al.*, *Nucleic Acids Res.* **41**, D203–D213 (2013).
13. L. Bintu *et al.*, *Curr. Opin. Genet. Dev.* **15**, 125–135 (2005).
14. T. Kuhlman, Z. Zhang, M. H. Saier Jr., T. Hwa, *Proc. Natl. Acad. Sci. U.S.A.* **104**, 6043–6048 (2007).
15. J. M. Vilar, S. Leibler, *J. Mol. Biol.* **331**, 981–989 (2003).
16. See supplementary materials on Science Online.
17. A. Sánchez, J. Kondev, *Proc. Natl. Acad. Sci. U.S.A.* **105**, 5081–5086 (2008).
18. P. S. Swain, M. B. Elowitz, E. D. Siggia, *Proc. Natl. Acad. Sci. U.S.A.* **99**, 12795–12800 (2002).
19. R. C. Brewster, D. L. Jones, R. Phillips, *PLoS Comput. Biol.* **8**, e1002811 (2012).
20. P. Hammar *et al.*, *Science* **336**, 1595–1598 (2012).
21. I. Golding, J. Paulsson, S. M. Zawilski, E. C. Cox, *Cell* **123**, 1025–1036 (2005).
22. A. Sanchez, S. Choubey, J. Kondev, *Annu. Rev. Biophys.* **42**, 469–491 (2013).
23. N. Mitarai, I. B. Dodd, M. T. Crooks, K. Sneppen, *PLoS Comput. Biol.* **4**, e1000109 (2008).

## ACKNOWLEDGMENTS

We thank H. J. Lee, C. Wiggins, Y. Lin, X. Zhu, F. Weinert, M. Rydenfelt, R. Milo, H. Garcia, N. Belliveau, and J. Sheung for

useful discussions. Supported by NIH grants DP1 OD000217 (Directors Pioneer Award), R01 GM085286, and 1 U54 CA143869 (Northwestern PSOC Center); La Fondation Pierre Gilles de Gennes (R.P.); and the Donna and Benjamin M. Rosen Center for Bioengineering at Caltech (D.L.J.). Raw microscopy image data are archived in the Phillips laboratory at Caltech and are available upon request.

## SUPPLEMENTARY MATERIALS

www.sciencemag.org/content/346/6216/1533/suppl/DC1  
Materials and Methods  
Supplementary Text  
Figs. S1 to S11  
Tables S1 to S3  
References (24–32)

28 April 2014; accepted 4 November 2014  
10.1126/science.1255301

## IMMUNE TOLERANCE

## Detection of self-reactive CD8<sup>+</sup> T cells with an anergic phenotype in healthy individuals

Yuka Maeda,<sup>1</sup> Hiroyoshi Nishikawa,<sup>1\*</sup> Daisuke Sugiyama,<sup>1</sup> Danbee Ha,<sup>1</sup> Masahide Hamaguchi,<sup>1</sup> Takuro Saito,<sup>1</sup> Megumi Nishioka,<sup>1,2</sup> James B. Wing,<sup>1</sup> Dennis Adeegbe,<sup>1</sup> Ichiro Katayama,<sup>2</sup> Shimon Sakaguchi<sup>1\*</sup>

Immunological tolerance to self requires naturally occurring regulatory T (T<sub>reg</sub>) cells. Yet how they stably control autoimmune T cells remains obscure. Here, we show that T<sub>reg</sub> cells can render self-reactive human CD8<sup>+</sup> T cells anergic (i.e., hypoproliferative and cytokine hypoproducing upon antigen restimulation) in vitro, likely by controlling the costimulatory function of antigen-presenting cells. Anergic T cells were naïve in phenotype, lower than activated T cells in T cell receptor affinity for cognate antigen, and expressed several coinhibitory molecules, including cytotoxic T lymphocyte-associated antigen-4 (CTLA-4). Using these criteria, we detected in healthy individuals anergic T cells reactive with a skin antigen targeted in the autoimmune disease vitiligo. Collectively, our results suggest that T<sub>reg</sub> cell-mediated induction of energy in autoimmune T cells is important for maintaining self-tolerance.

Naturally occurring CD25<sup>+</sup>CD4<sup>+</sup> regulatory T (T<sub>reg</sub>) cells, which specifically express the transcription factor FoxP3, actively maintain immunological self-tolerance and homeostasis (1). Developmental or functional anomalies of natural T<sub>reg</sub> cells can cause autoimmune diseases (such as type I diabetes), allergy, and immunopathological diseases (such as inflammatory bowel disease) (2). How T<sub>reg</sub> cells effectively control potentially hazardous self-reactive T cells in humans remains an open question. In particular, it is unknown whether T<sub>reg</sub> cell-mediated suppression for a limited period has a critical long-lasting effect on cell fate and antigen reactivity of autoimmune T cells.

To address this issue, we examined proliferation, cytokine production, and cell fate of antigen-

specific CD8<sup>+</sup> T cells in peripheral blood mononuclear cells (PBMCs) from healthy individuals stimulated in vitro with self-antigen peptide in the presence or absence of natural FoxP3<sup>+</sup>CD25<sup>+</sup>CD4<sup>+</sup> T<sub>reg</sub> cells. Melan-A (also known as MART-1) used in the experiments is a self-antigen expressed by normal melanocytes and some melanoma cells and targeted in vitiligo vulgaris, an autoimmune disease of the skin (2–5). In the absence of T<sub>reg</sub> cells, Melan-A-specific CD8<sup>+</sup> T cells [detectable by major histocompatibility complex (MHC) tetramers and peptide tetramers] expanded over 10 days from very few cells to a sizable fraction when cultured with peptide-pulsed autologous antigen-presenting cells (APCs) (Fig. 1A) (6). Natural T<sub>reg</sub> cells, which appeared to be activated by endogenous self-peptides and class II MHC on autologous APCs (7–9), suppressed the expansion of Melan-A tetramer-positive (Tet<sup>+</sup>) CD8<sup>+</sup> T cells in a dose-dependent manner. Similar stimulation with irrelevant peptide NY-ESO-1, another self- and tumor antigen, failed to induce Melan-A Tet<sup>+</sup>CD8<sup>+</sup> T cells. In cultures containing T<sub>reg</sub> cells,

<sup>1</sup>Experimental Immunology, Immunology Frontier Research Center (IFReC-WPI), Osaka University, Osaka 565-0871, Japan.

<sup>2</sup>Department of Dermatology, Graduate School of Medicine, Osaka University, Osaka 565-0871, Japan.

\*Corresponding author. E-mail: shimon@ifrec.osaka-u.ac.jp (S.S.); nisihiro@ifrec.osaka-u.ac.jp (H.N.)



we noted an accumulation of Tet<sup>+</sup>CD8<sup>+</sup> T cells that had divided once and then stopped further proliferation. This proliferation-aborted population increased in ratio, whereas the population under multiple cell divisions reciprocally decreased, in proportion to the number of added T<sub>reg</sub> cells. The proliferation-aborted cells had significantly lower tetramer staining intensity than the cells that had vigorously proliferated in the absence of T<sub>reg</sub> cells (peak a versus b in Fig. 1A, Fig. 1B, and fig. S1). The staining intensity of T cell receptor- $\alpha\beta$  (TCR- $\alpha\beta$ ) chains was equivalent in both populations, which indicated that the lower tetramer staining intensity was not due to down-modulation of TCR but to lower TCR affinity for the Melan-A peptide, as supported by significantly lower ratios of tetramer versus TCR- $\alpha\beta$  staining

intensities (Fig. 1C). Functionally, they produced reduced levels of cytokines such as interferon- $\gamma$  (IFN- $\gamma$ ), tumor necrosis factor- $\alpha$  (TNF- $\alpha$ ), and interleukin 2 (IL-2) (Fig. 1, D and E), despite the addition of exogenous IL-2 to maintain cultured T cells. Furthermore, upon secondary stimulation, they remained hypoproliferative and produced very low amounts of cytokines (fig. S2). Thus, antigenic stimulation under T<sub>reg</sub> cell-mediated suppression allows responder T cells with relatively low affinity TCRs for a self-antigen to divide once but prevents their further proliferation, which drives them into a profoundly and stably hypoproliferative and cytokine-hypoproducing state, which can be immunologically defined as “anergy” (10–13).

In contrast with anti-Melan-A responses, CD8<sup>+</sup> T cells from the same donor, who had detectable

serum anticytomegalovirus (CMV) immunoglobulin G (IgG) antibody, had CMV peptide-specific T cells with a memory phenotype (fig. S3, A to D). CMV-specific CD8<sup>+</sup> T cells, whether they were in a naïve or memory cell fraction, vigorously proliferated and produced inflammatory cytokines even at a high T<sub>reg</sub>-to-responder T cell ratio, with no significant differences in CMV tetramer staining intensity among CD8<sup>+</sup> T cells proliferating in the presence or absence of T<sub>reg</sub> cells (fig. S3, E to H). However, high numbers of T<sub>reg</sub> cells completely inhibited the proliferation of polyclonally activated naïve CD8<sup>+</sup> T cells without allowing a single cell division (fig. S4). The nondividing CD8<sup>+</sup> T cells proliferated as actively as nonsuppressed cells upon restimulation after removal of T<sub>reg</sub> cells.

Collectively, T<sub>reg</sub>-cell dosage, the immunological states of responder T cells (e.g., in a naïve or memory state), and their TCR affinity for cognate antigen contribute to T<sub>reg</sub> cell-mediated induction of anergy. This is an active process and differs from a mere naïve nonproliferative state.

Microarray gene expression analysis revealed that activated or anergic Tet<sup>+</sup>CD8<sup>+</sup> T cells or Tet<sup>+</sup>CD8<sup>+</sup> T cells obtained from T<sub>reg</sub>-absent or -present cell cultures were substantially different in gene expression profiles (Fig. 2A). As the most striking differences, the transcription of *CTLA4*, encoding the coinhibitory molecule CTLA-4 (14), was significantly up-regulated, whereas *BCL2*, encoding the apoptosis-inhibiting molecule B cell lymphoma-2 (BCL-2) (15), was down-regulated in anergic CD8<sup>+</sup> T cells, as confirmed by quantitative reverse transcription polymerase chain reaction (RT-PCR) (Fig. 2B). There were no significant differences in the expression of *PDCDI* encoding the coinhibitory molecule PD-1; the genes encoding the anergy-related molecules *GRAIL*, *CBL-B*, and *EGR-2* (16–19); *BAT3*, *TBX21*, and *EOMES*, putative markers for exhausted CD8<sup>+</sup> T cells (20, 21); and *p27KIP1*, a cyclin-dependent kinase inhibitor. Anergic CD8<sup>+</sup> T cells did not express *FoxP3* (Fig. 2B and fig. S5A). The majority (>90%) of anergic CD8<sup>+</sup> T cells expressed both CTLA-4 and the chemokine receptor CCR7, which differed from the phenotype of activated or naïve CD8<sup>+</sup> T cells (Fig. 2, C and D, and fig. S5, B to D) (22, 23). Functionally, during secondary stimulation of anergic Tet<sup>+</sup>CD8<sup>+</sup> T cells with Melan-A peptide-pulsed APCs after removal of T<sub>reg</sub> cells, antibody blockade of CTLA-4 and PD-1 at doses enhancing cytokine production by activated conventional T cells failed to rescue proliferation resistance or cytokine hypoproduction of anergic CD8<sup>+</sup> T cells (fig. S5E) (24). Addition of a high dose of IL-2 induced apoptosis in restimulated Tet<sup>+</sup>CD8<sup>+</sup> T cells rather than abrogating their hyporesponsiveness. Nevertheless, anergic CD8<sup>+</sup> T cells were not in the process of immediate apoptosis (fig. S6), despite their lower *BCL2* expression than activated T cells (Fig. 2B). Thus, anergic CD8<sup>+</sup> T cells induced by T<sub>reg</sub> cell-mediated suppression are distinct from activated or naïve T cells in gene and protein expression profiles. They also appear to be different from “exhausted” CD8<sup>+</sup> T cells, which develop as PD-1<sup>+</sup> hypoproliferative and cytokine-hypoproducing cells

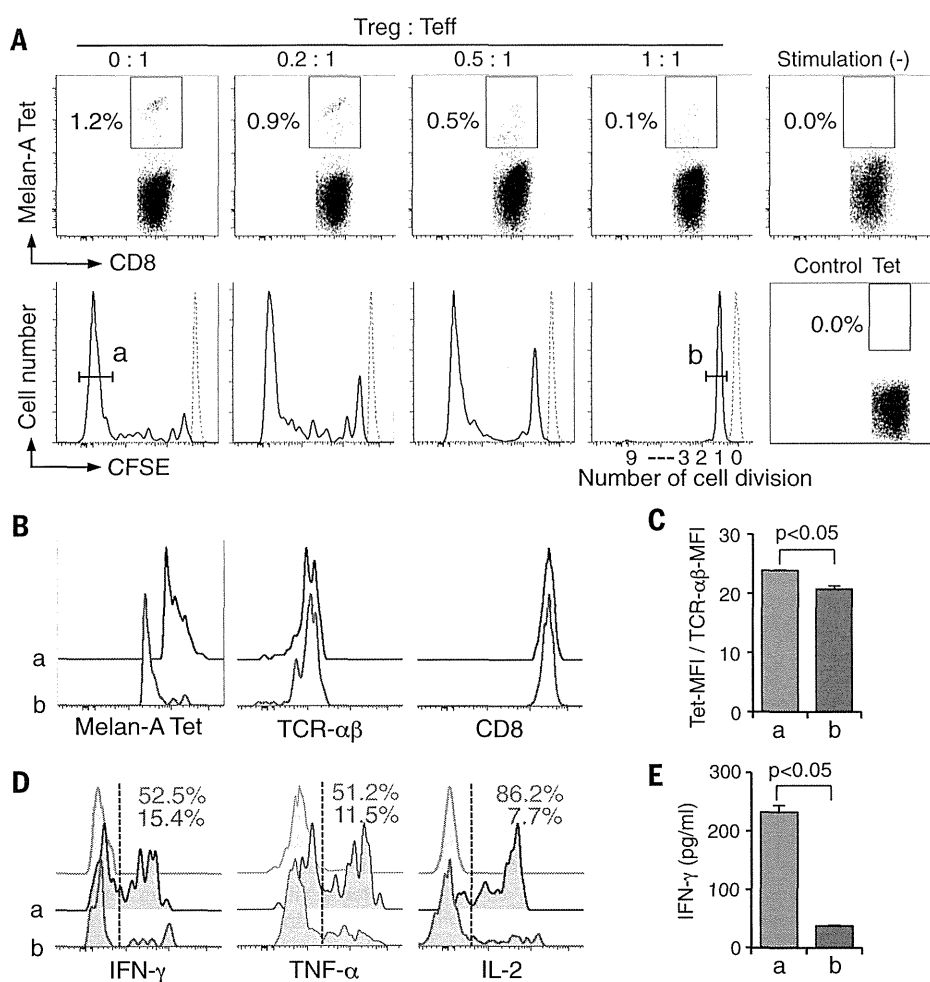


**Fig. 1. Natural T<sub>reg</sub> cells render low-affinity self-reactive CD8<sup>+</sup> T cells anergic upon antigen stimulation.** (A) Melan-A-specific CD8<sup>+</sup> T cell induction. CFSE-labeled CD8<sup>+</sup> T cells of HLA-A\*0201<sup>+</sup> healthy individuals were stimulated by T cell-depleted,  $\gamma$ -irradiated, and Melan-A<sub>26-35</sub> peptide-pulsed APCs with graded numbers of CD25<sup>high</sup>CD4<sup>+</sup> T<sub>reg</sub> cells for 10 days (6). Dotted lines mean Tet<sup>+</sup>CD8<sup>+</sup> cells showing no CFSE dilution. Control tet: NY-ESO-1<sub>157-165</sub>/HLA-A\*0201 tetramer. T<sub>eff</sub> refers to CD8<sup>+</sup> effector T cells. (B) Tet, TCR- $\alpha\beta$ , and CD8 staining of Tet<sup>+</sup>CD8<sup>+</sup> T cells. Results in (A) and (B) are representative of 10 independent experiments. (C) Relative tetramer staining intensities, calculated as mean fluorescence intensity (MFI) of Tet/MFI of TCR- $\alpha\beta$  staining of Tet<sup>+</sup>CD8<sup>+</sup> T cells ( $n = 5$ ). (D and E) Cytokine production of Tet<sup>+</sup>CD8<sup>+</sup> T cells by intracellular staining (D) and enzyme-linked immunosorbent assay (E) (6). Representative result of three independent experiments. The labels a and b in (B) to (E) mean the cell accumulations like a or b in (A). Error bars indicate means  $\pm$  SEM. The significance was assessed by Student's two-tailed paired  $t$  test.

in chronic viral infections and in tumor tissues, because exhausted CD8<sup>+</sup> T cells are reportedly CCR7<sup>-</sup>, CD45RA<sup>-</sup>, and BAT3<sup>+</sup>, and their exhaustion can be rescued by a PD-1-blocking antibody (21, 24–26).

T<sub>reg</sub> cells suppress the activation and/or proliferation of responder T cells (27), at least in part, by down-regulating the expression of the costimulatory molecules CD80 and CD86 on APCs (fig. S7A) (28, 29). To determine whether low expression or down-modulation of CD80 and CD86 on dendritic cells (DCs) was responsible for the induction of antigen-specific anergic CD8<sup>+</sup> T cells, we stimulated carboxyfluorescein succinimidyl ester (CFSE)-labeled CD8<sup>+</sup> T cells with autologous immature or mature DCs pulsed with Melan-A

peptide in the presence of graded amounts of CTLA-4-immunoglobulin (CTLA-4Ig), which blocked CD80 and CD86 (fig. S7B) (30). In contrast to the vigorous proliferation of Tet<sup>+</sup>CD8<sup>+</sup> T cells cultured with mature DCs, the majority of Tet<sup>+</sup>CD8<sup>+</sup> T cells generated with immature DCs, and some with mature DCs with a high dose (100 μg/ml) of CTLA-4Ig, were proliferation-aborted after one cell division (Fig. 3A). The proliferation-aborted T cells (peaks c and d in Fig. 3A) were lower than proliferating T cells in Melan-A tetramer staining intensity (Fig. 3B), and highly expressed CTLA-4 and CCR7 (fig. S7, C and D); they formed a discrete CTLA-4/CCR7 double-positive population (Fig. 3C and fig. S7E). They produced significantly lower amounts of IFN-γ,

TNF-α, and IL-2 compared with Tet<sup>+</sup>CD8<sup>+</sup> cells, having proliferated in culture with mature DCs (fig. S7F). Similar to peptide stimulation, polyclonal antibody against CD3-specific monoclonal antibody (mAb) stimulation of CTLA-4<sup>-</sup> naïve CD8<sup>+</sup> T cells in the presence of CTLA-4Ig produced cells that were proliferation-aborted after one cell division (fig. S8A). Notably, increasing CTLA-4Ig dose proportionally intensified CTLA-4 expression by the aborted cells, while stably maintaining their high CCR7 expression (fig. S8, A and B). Taken together, antigen presentation with low CD80 and CD86 costimulation is able to drive CD8<sup>+</sup> T cells to differentiate into CTLA-4<sup>+</sup>CCR7<sup>+</sup> anergic cells. DCs with moderate CD80 and CD86 reduction can concurrently generate both

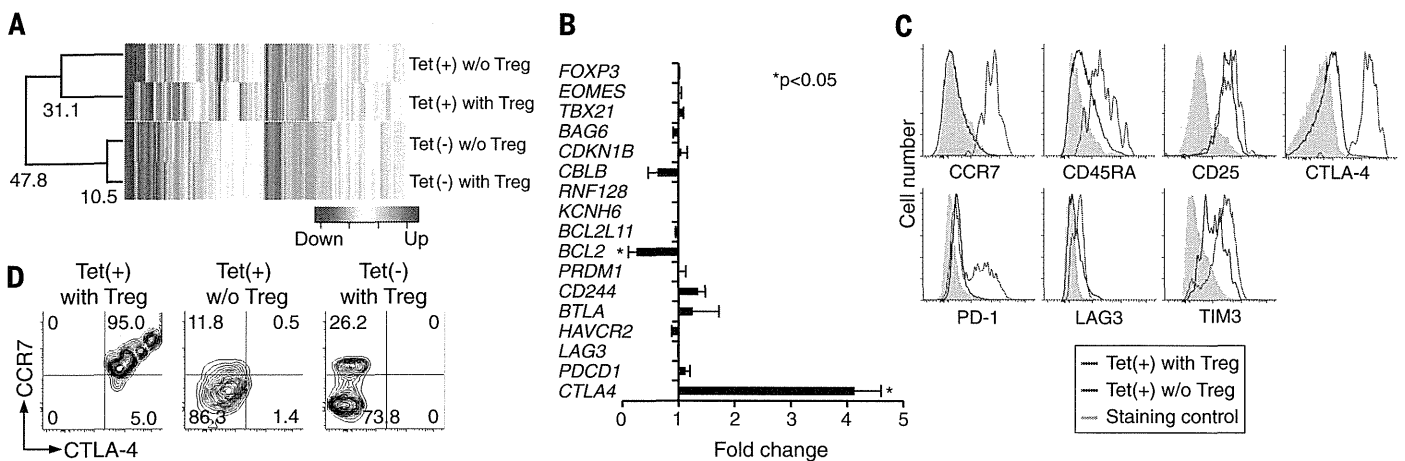


**Fig. 2. Distinct phenotype and function of anergic CD8<sup>+</sup> T cells produced by T<sub>reg</sub> cell suppression.** (A) Global mRNA expression profile. Tet<sup>+</sup>CD8<sup>+</sup> T cells induced at CD8<sup>+</sup> T cells: T<sub>reg</sub> cell ratios of 1:0.5 and 1:0 were subjected to microarray analyses. Gene expression reportedly associated with CD8<sup>+</sup> T cell function was compared among the indicated four groups and expressed as a heat map. Correlation distances shown were calculated by h-clust (6). Representative of two independent experiments. (B) mRNA expression measured by

quantitative real-time PCR. Fold changes of mRNA level as [Tet(+)] with T<sub>reg</sub>] versus [Tet(+)] without T<sub>reg</sub>] in five independent experiments are shown. Error bars indicate means ± SEM. (C and D) Expression of cell surface molecules by Tet<sup>+</sup>CD8<sup>+</sup> T cells induced at CD8<sup>+</sup> T cells: T<sub>reg</sub> cell ratios, 1:1 and 1:0. Representative histogram staining pattern (C) and contour plot staining pattern of CTLA-4 and CCR7 (D). Data are representative of five independent experiments (n = 10). The significance was assessed by Student's two-tailed paired t test.

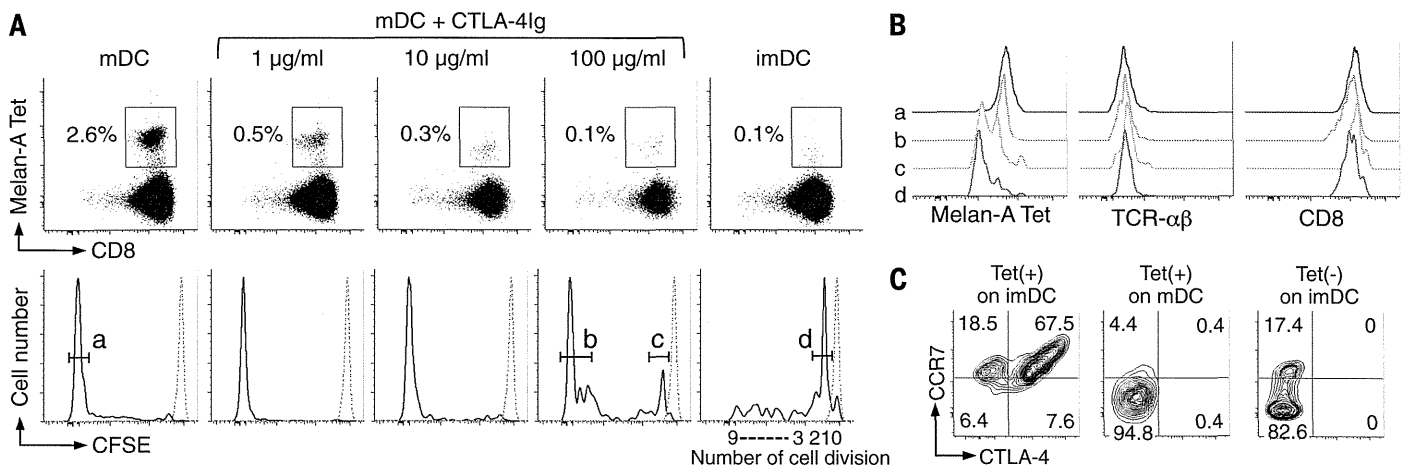


**Fig. 3. DC expression of CD80 and CD86 controls the generation of CTLA-4<sup>+</sup>CCR7<sup>+</sup> low-affinity anergic self-reactive T cells.** (A) Melan-A-specific CD8<sup>+</sup> T cell induction. CFSE-labeled CD8<sup>+</sup> T cells of HLA-A\*0201<sup>+</sup> healthy individuals were stimulated with γ-irradiated, Melan-A<sub>26-35</sub> peptide-pulsed monocyte-derived immature or mature DCs. CTLA-4Ig was added into mature DCs cultures at indicated concentrations (6). (B) Tet, TCR-αβ, and CD8 staining intensity of Tet<sup>+</sup>CD8<sup>+</sup> T cells shown in (A). (C) Representative contour plot staining pattern of Tet<sup>+</sup> or Tet<sup>-</sup>CD8<sup>+</sup> T cells shown in (A) for CTLA-4 and CCR7. Data in (A) to (C) are representative of five independent experiments.



activated T cells and anergic T cells, in part, depending on TCR affinity.

The above *in vitro* findings prompted us to ask whether healthy individuals harbored such anergic self-reactive CD8<sup>+</sup> T cells. Direct *ex vivo* staining of CD8<sup>+</sup> T cells in PBMCs of healthy donors ( $n = 10$ ) for Melan-A peptide and MHC tetramer, with CD8<sup>+</sup> T cells from vitiligo patients ( $n = 10$ ) as a positive control, revealed that a small number of Tet<sup>+</sup>CD8<sup>+</sup> T cells were indeed present in healthy individuals and constituted ~0.03% of CD8<sup>+</sup> T cells in PBMCs, which contrasted with high percentages (~0.1%) in vitiligo patients (Fig. 4, A and B) (6). Two-thirds of the former had a naïve

(CCR7<sup>+</sup>CD45RA<sup>+</sup>) phenotype, whereas the majority of the latter had an effector or memory phenotype (Fig. 4C and fig. S9A) (4, 5). The Tet<sup>+</sup>CD8<sup>+</sup> T cells from healthy individuals had significantly lower tetramer staining intensity than those from vitiligo patients (Fig. 4, D and E). They expressed CTLA-4 at higher levels than Tet<sup>+</sup>CD8<sup>+</sup> T cells from vitiligo patients or Tet<sup>-</sup>CD8<sup>+</sup> T cells from healthy individuals, or activated CD8<sup>+</sup> T or natural T<sub>reg</sub> cells (Fig. 4F and fig. S9, B to D), and ~90% of the Tet<sup>+</sup>CD45RA<sup>+</sup>CD8<sup>+</sup> cells were double positive for CTLA-4 and CCR7 (Fig. 4G and fig. S9B). Functionally, Tet<sup>+</sup>CD8<sup>+</sup> T cells directly prepared from healthy donors scarcely

produced IFN- $\gamma$ , TNF- $\alpha$ , or IL-2, contrasting with active cytokine production by naïve Tet<sup>-</sup>CD8<sup>+</sup> T cells (Fig. 4H) or Melan-A-specific CD8<sup>+</sup> T cells from vitiligo patients (4, 3I).

To determine further the function of these anergic T cells, we cocultured CTLA-4<sup>+</sup> and CTLA-4<sup>-</sup> fractions of naïve (CCR7<sup>+</sup>CD45RA<sup>+</sup>) CD8<sup>+</sup> T cells from healthy individuals and assessed the proliferative activity of Tet<sup>+</sup>CD8<sup>+</sup> T cells present in each fraction (Fig. 4I). The CTLA-4<sup>-</sup> fraction, which constituted less than 10% of naïve CD8<sup>+</sup> T cells in healthy donors, contained the majority (~95%) of Melan-A Tet<sup>+</sup>CD8<sup>+</sup> T cells before stimulation (Fig. 4, I to K). These CTLA-4<sup>+</sup>Tet<sup>+</sup> cells were

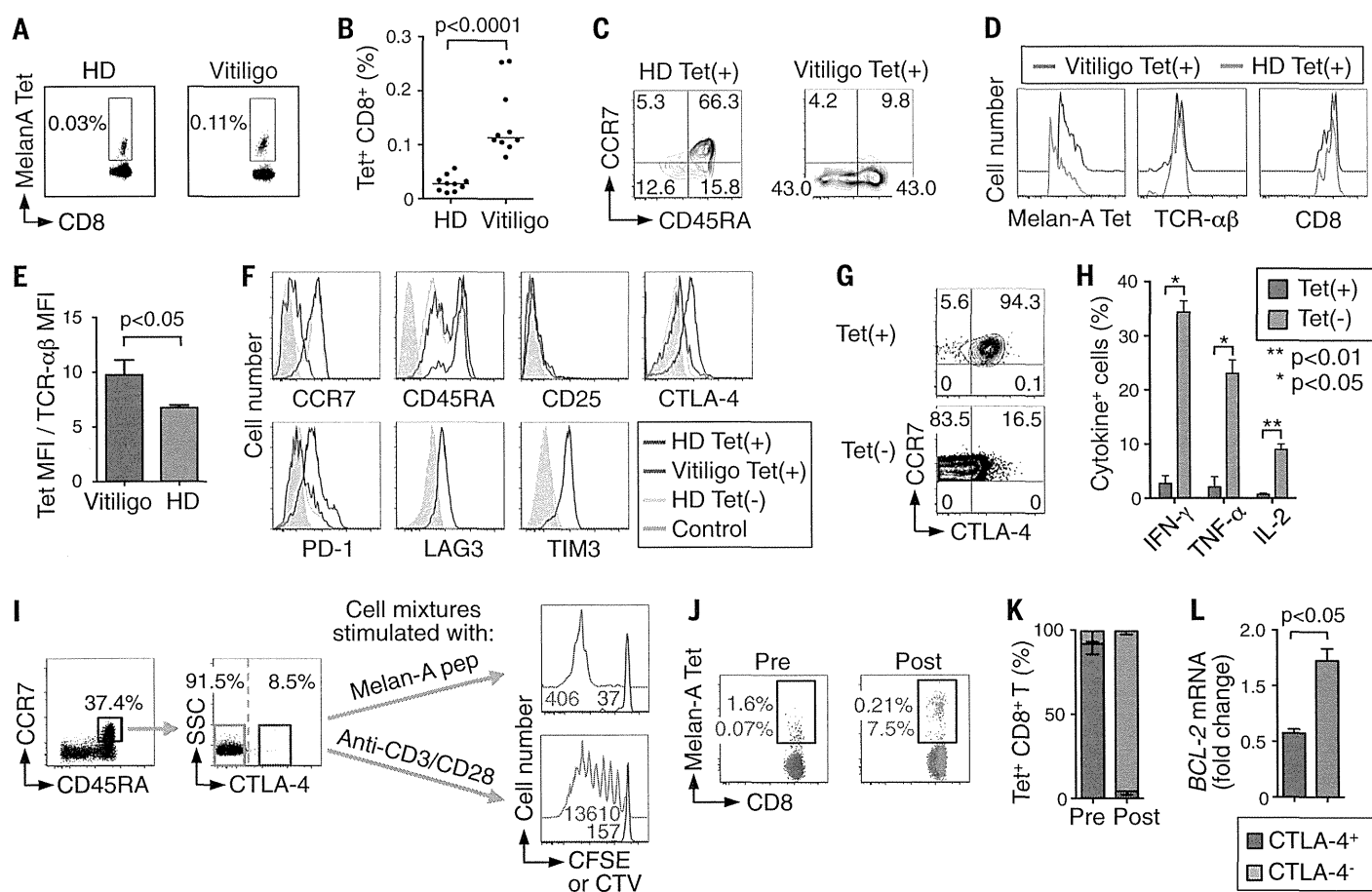


**Fig. 4. Detection of low-affinity anergic self-reactive CTLA-4<sup>+</sup>CCR7<sup>+</sup>CD8<sup>+</sup> T cells in healthy individuals.** (A) Melan-A Tet<sup>+</sup>CD8<sup>+</sup> T cells in PBMCs of a healthy donor (HD) and a vitiligo patient. (B) Percentages of Tet<sup>+</sup>CD8<sup>+</sup> T cells in HDs and vitiligo patients ( $n = 10$ ). (C) CCR7 and CD45RA expression by Tet<sup>+</sup>CD8<sup>+</sup> T cells in an HD and a vitiligo patient. (D) Tet, TCR- $\alpha$ , and CD8 staining intensity of Tet<sup>+</sup>CD8<sup>+</sup> T cells in an HD and a vitiligo patient. (E) Ratios of MFI of tetramer staining to MFI of TCR- $\alpha$  staining in Tet<sup>+</sup>CD8<sup>+</sup> T cells in HDs and vitiligo patients ( $n = 4$  each). (F) Expression of cell surface molecules by Tet<sup>+</sup> or Tet<sup>-</sup>CD8<sup>+</sup> T cells in a representative HD and a vitiligo patient. (G) Representative staining for CTLA-4 and CCR7 of Tet<sup>+</sup> or Tet<sup>-</sup> cells in CD45RA<sup>+</sup>CD8<sup>+</sup> T cells of an HD. Data shown in (A), (C), (D), (F), and (G) are representative of four independent experiments. (H) Cytokine production by Tet<sup>+</sup>CD8<sup>+</sup> T cells in HDs assessed by intracellular staining with CCR7<sup>+</sup>CD45RA<sup>+</sup>Tet<sup>+</sup>CD8<sup>+</sup> T cells as control. Data summarize four independent experiments. (I) Proliferation and cytokine production of CTLA-4<sup>+</sup> or CTLA-4<sup>-</sup> naïve CD8<sup>+</sup> T cells in HDs. CCR7<sup>+</sup>CD45RA<sup>+</sup>CD8<sup>+</sup> T cells

from HD PBMCs were further separated into CTLA-4<sup>+</sup> and CTLA-4<sup>-</sup> cells, labeled with Cell Trace Violet (CTV) or CFSE, respectively, mixed at a 1:1 ratio, stimulated with Melan-A<sub>26-35</sub> peptide-pulsed APCs for 10 days (top) or CD3/CD28-specific mAb for 5 days (bottom), and assessed for proliferation by CTV or CFSE dilution (red and blue, respectively) (6). Numbers in right two figures represent the numbers of cells in each cell fraction. SSC, side scatter. (J) Representative tetramer staining of the cell mixtures before (Pre) and after (Post) Melan-A<sub>26-35</sub> peptide stimulation for 10 days. Numbers represent percentages of Tet<sup>+</sup>CD8<sup>+</sup> cells in the CTLA-4<sup>+</sup> or CTLA-4<sup>-</sup> fraction (red and blue, respectively). (K) Percentages of Tet<sup>+</sup>CD8<sup>+</sup> T cells in the CTLA-4<sup>+</sup> (red) or CTLA-4<sup>-</sup> (blue) fraction in the cell mixtures before (Pre) and after (Post) cell culture as shown in (I) and (J). (L) *BCL2* mRNA expression of CTLA-4<sup>+</sup>CCR7<sup>+</sup>CD45RA<sup>+</sup>Tet<sup>+</sup>CD8<sup>+</sup> and CTLA-4<sup>-</sup>CCR7<sup>+</sup>CD45RA<sup>+</sup>Tet<sup>+</sup>CD8<sup>+</sup> T cells measured by quantitative real-time PCR. Data in (I) to (L) are representative of at least three independent experiments. Error bars indicate means  $\pm$  SEM. The significance was assessed by Student's two-tailed paired *t* test.

hypoproliferative, low in *BCL2* expression, and prone to die upon Melan-A stimulation (Fig. 4, I to L). In contrast, the CTLA-4<sup>-</sup> fraction, which initially contained fewer than 5% of total Tet<sup>+</sup>CD8<sup>+</sup> T cells, gave rise to proliferating Tet<sup>+</sup>CD8<sup>+</sup> T cells, which made up ~95% of total Tet<sup>+</sup>CD8<sup>+</sup> T cells after stimulation (Fig. 4, I to K). In addition, polyclonal stimulation of the cell mixtures with CD3-specific and CD28-specific mAb revealed that the CTLA-4<sup>+</sup> fraction as a whole was hypoproliferative (Fig. 4I) and cytokine hypoproducing (fig. S9E), in contrast with active proliferation and cytokine production of the CTLA-4<sup>-</sup> fraction.

These results collectively indicate that healthy individuals harbor at least two distinct populations of self-reactive CD8<sup>+</sup> T cells: one that is functionally anergic and expresses CTLA-4 and CCR7 and another that is CTLA-4<sup>-</sup> and naïve in function and phenotype. The latter, especially those with high-affinity TCRs, may become activated and expand upon self-antigen stimulation in the absence or reduction of natural T<sub>reg</sub> cells, as shown in Fig. 1A.

Thus, anergic self-reactive T cells, which are phenotypically distinct from other T cells, are physiologically present in the immune system. They appear to be generated, at least in part, as a result of T<sub>reg</sub>-mediated suppression, which can determine cell fate of responder T cells (i.e., activated, anergic, or ignorant) upon antigenic stimulation, depending on the number and suppressive activity of T<sub>reg</sub> cells, the TCR affinity and differentiation states of responder T cells, and the condition of APCs. This T<sub>reg</sub>-dependent switching of re-

sponder T cell fate can be a key target in controlling autoimmunity and tumor immunity, as illustrated by our analysis of Melan-A-specific immune responses, as well as a variety of other physiological and pathological immune responses.

#### REFERENCES AND NOTES

1. S. Sakaguchi, *Nat. Immunol.* **6**, 345–352 (2005).
2. P. G. Coulie et al., *J. Exp. Med.* **180**, 35–42 (1994).
3. Y. Kawakami et al., *Proc. Natl. Acad. Sci. U.S.A.* **91**, 6458–6462 (1994).
4. G. S. Ogg, P. Rod Dunbar, P. Romero, J. L. Chen, V. Cerundolo, *J. Exp. Med.* **188**, 1203–1208 (1998).
5. M. J. Pittet et al., *J. Exp. Med.* **190**, 705–716 (1999).
6. Materials and methods are available as supplementary materials on Science Online.
7. M. Itoh et al., *J. Immunol.* **162**, 5317–5326 (1999).
8. C. S. Hsieh, H. M. Lee, C. W. Lio, *Nat. Rev. Immunol.* **12**, 157–167 (2012).
9. T. Yamaguchi et al., *Proc. Natl. Acad. Sci. U.S.A.* **110**, E2116–E2125 (2013).
10. M. K. Jenkins, R. H. Schwartz, *J. Exp. Med.* **165**, 302–319 (1987).
11. R. H. Schwartz, *Annu. Rev. Immunol.* **21**, 305–334 (2003).
12. F. Macián, S. H. Im, F. J. García-Cózar, A. Rao, *Curr. Opin. Immunol.* **16**, 209–216 (2004).
13. A. D. Wells, *J. Immunol.* **182**, 7331–7341 (2009).
14. A. H. Sharpe, G. J. Freeman, *Nat. Rev. Immunol.* **2**, 116–126 (2002).
15. P. E. Czabotar, G. Lessene, A. Strasser, J. M. Adams, *Nat. Rev. Mol. Cell Biol.* **15**, 49–63 (2014).
16. N. Anandasabapathy et al., *Immunity* **18**, 535–547 (2003).
17. M. S. Jeon et al., *Immunity* **21**, 167–177 (2004).
18. D. L. Mueller, *Nat. Immunol.* **5**, 883–890 (2004).
19. Y. Zheng, Y. Zha, G. Driessens, F. Locke, T. F. Gajewski, *J. Exp. Med.* **209**, 2157–2163 (2012).
20. M. A. Paley et al., *Science* **338**, 1220–1225 (2012).
21. M. Rangachari et al., *Nat. Med.* **18**, 1394–1400 (2012).
22. F. Sallusto, D. Lenig, R. Förster, M. Lipp, A. Lanzavecchia, *Nature* **401**, 708–712 (1999).
23. M. A. Williams, M. J. Bevan, *Annu. Rev. Immunol.* **25**, 171–192 (2007).
24. D. L. Barber et al., *Nature* **439**, 682–687 (2006).
25. S. D. Blackburn et al., *Nat. Immunol.* **10**, 29–37 (2009).
26. E. J. Wherry, *Nat. Immunol.* **12**, 492–499 (2011).
27. E. M. Shevach, *Immunity* **30**, 636–645 (2009).
28. K. Wing et al., *Science* **322**, 271–275 (2008).
29. O. S. Qureshi et al., *Science* **332**, 600–603 (2011).
30. J. A. Bluestone, E. W. St. Clair, L. A. Turka, *Immunity* **24**, 233–238 (2006).
31. K. S. Lang et al., *J. Invest. Dermatol.* **116**, 891–897 (2001).

#### ACKNOWLEDGMENTS

We thank Y. Tada, K. Teshima, and Y. Funabiki for technical assistance. The data presented in this paper are tabulated in the main paper and in the supplementary materials. Microarray data are deposited in GSE63129. This study was supported by Grants-in-Aid for Specially Promoted Research (to S.S., no. 20002007) and for Scientific Research (i) (to S.S., no. 26253030) and (ii) (to H.N., no. 23300354 and 26290054) from the Ministry of Education, Culture, Sports, Science, and Technology of Japan; Core Research for Evolutional Science and Technology (CREST) from Japan Science and Technology Agency (to S.S.); Health and Labor Sciences Research Grants, Research on Applying Health Technology (H24-Clinical Cancer Research-general-006 to H.N.) from the Ministry of Health, Labor, and Welfare, Japan, the Cancer Research Institute CLIP grant to H.N. All authors have no competing financial interest.

#### SUPPLEMENTARY MATERIALS

[www.sciencemag.org/content/346/6216/1536/suppl/DC1](http://www.sciencemag.org/content/346/6216/1536/suppl/DC1)

Materials and Methods

Supplemental Text

Figs. S1 to S9

References (32–37)

21 October 2014; accepted 20 November 2014

10.1126/science.aal1292

# Interleukin-10-Producing Plasmablasts Exert Regulatory Function in Autoimmune Inflammation

Masanori Matsumoto,<sup>1,4</sup> Akemi Baba,<sup>1</sup> Takafumi Yokota,<sup>5</sup> Hiroyoshi Nishikawa,<sup>2</sup> Yasuyuki Ohkawa,<sup>7</sup> Hisako Kayama,<sup>3,6</sup> Axel Kallies,<sup>8,9</sup> Stephen L. Nutt,<sup>8,9</sup> Shimon Sakaguchi,<sup>2</sup> Kiyoshi Takeda,<sup>3,6</sup> Tomohiro Kurosaki,<sup>1,4,\*</sup> and Yoshihiro Baba<sup>1,4,\*</sup>

<sup>1</sup>Laboratory for Lymphocyte Differentiation

<sup>2</sup>Laboratory for Experimental Immunology

<sup>3</sup>Laboratory for Immune Regulation

WPI Immunology Frontier Research Center, Osaka University, Suita, Osaka 565-0871, Japan

<sup>4</sup>Laboratory for Lymphocyte Differentiation, RIKEN Center for Integrative Medical Sciences (IMS), Yokohama, Kanagawa 230-0045, Japan

<sup>5</sup>Department of Hematology and Oncology

<sup>6</sup>Department of Microbiology and Immunology

Graduate School of Medicine, Osaka University, Suita, Osaka 565-0871, Japan

<sup>7</sup>Department of Advanced Medical Initiatives, JST-CREST, Faculty of Medicine, Kyushu University, Fukuoka 812-8582, Japan

<sup>8</sup>The Walter and Eliza Hall Institute of Medical Research, Parkville, VIC 3050, Australia

<sup>9</sup>Department of Medical Biology, The University of Melbourne, Parkville, VIC 3010, Australia

\*Correspondence: kurosaki@ifrec.osaka-u.ac.jp (T.K.), babay@ifrec.osaka-u.ac.jp (Y.B.)

<http://dx.doi.org/10.1016/j.immuni.2014.10.016>

## SUMMARY

B cells can suppress autoimmunity by secreting interleukin-10 (IL-10). Although subpopulations of splenic B lineage cells are reported to express IL-10 *in vitro*, the identity of IL-10-producing B cells with regulatory function *in vivo* remains unknown. By using IL-10 reporter mice, we found that plasmablasts in the draining lymph nodes (dLNs), but not splenic B lineage cells, predominantly expressed IL-10 during experimental autoimmune encephalomyelitis (EAE). These plasmablasts were generated only during EAE inflammation. Mice lacking plasmablasts by genetic ablation of the transcription factors Blimp1 or IRF4 in B lineage cells developed an exacerbated EAE. Furthermore, IRF4 positively regulated IL-10 production that can inhibit dendritic cell functions to generate pathogenic T cells. Our data demonstrate that plasmablasts in the dLNs serve as IL-10 producers to limit autoimmune inflammation and emphasize the importance of plasmablasts as IL-10-producing regulatory B cells.

## INTRODUCTION

In the context of autoimmune disorders, B cells can be pathogenic effectors through their production of autoantibodies. However, evidence is accumulating that B cells can also be immunosuppressive in T-cell-mediated autoimmune and inflammatory diseases. Examples are collagen-induced arthritis (CIA) (Mauri et al., 2003), systemic lupus erythematosus (SLE) (Watanabe et al., 2010), and experimental autoimmune encephalomyelitis (EAE), an animal model of human multiple sclerosis

(MS) (Fillatreau et al., 2002; Matsushita et al., 2008). The regulatory function of B cells is considered to be mainly determined by the secretion of interleukin-10 (IL-10), which is controlled by signals from Toll-like receptors (TLRs) (Lampropoulou et al., 2008), CD40 (Mauri et al., 2003), and B cell antigen receptors (BCR) (Fillatreau et al., 2002). To date, several unique populations of splenic IL-10-competent B cells (regulatory B cells) have been described. They include CD21<sup>hi</sup>CD23<sup>hi</sup>IgM<sup>hi</sup> transitional 2-marginal zone precursor (T2-MZP) B cells (Evans et al., 2007) and CD1d<sup>hi</sup>CD5<sup>+</sup> B cells (Matsushita et al., 2008) that have been reported to inhibit autoimmunity. In addition, splenic CD138<sup>+</sup> plasma cells were also reported to express IL-10 (Shen et al., 2014). However, these populations produce detectable IL-10 only when stimulated *ex vivo*. Thus, despite progress made in understanding the importance of B-cell-derived IL-10, there has been no definitive identification of *in vivo* IL-10-producing B cells with regulatory function during autoimmunity.

In humans, a role for B-cell-derived IL-10 in downregulation of inflammatory reactions has been suggested in autoimmune diseases such as MS or SLE (Blair et al., 2010; Duddy et al., 2007; Mauri and Bosma, 2012). Treatment with rituximab for B cell depletion efficiently ameliorated the disease progression in some autoimmune diseases, presumably because of elimination of pathogenic B cells (Gürcan et al., 2009). However, this might work in part because of selective survival and repopulation of regulatory B cell subsets (Duddy et al., 2007; Todd et al., 2014). The functional and clinical importance of human IL-10-competent B cells has begun to be elucidated but more must be learned about their characteristics.

Here we have exploited IL-10 reporter mice to identify *in vivo* IL-10-producing B cells and demonstrate that CD138<sup>+</sup> plasmablasts, proliferating immature plasma cells, are the predominant source of IL-10 during EAE development. IL-10-producing plasmablasts were generated specifically in the draining lymph nodes (dLNs) but not in the spleen after EAE induction. By genetic

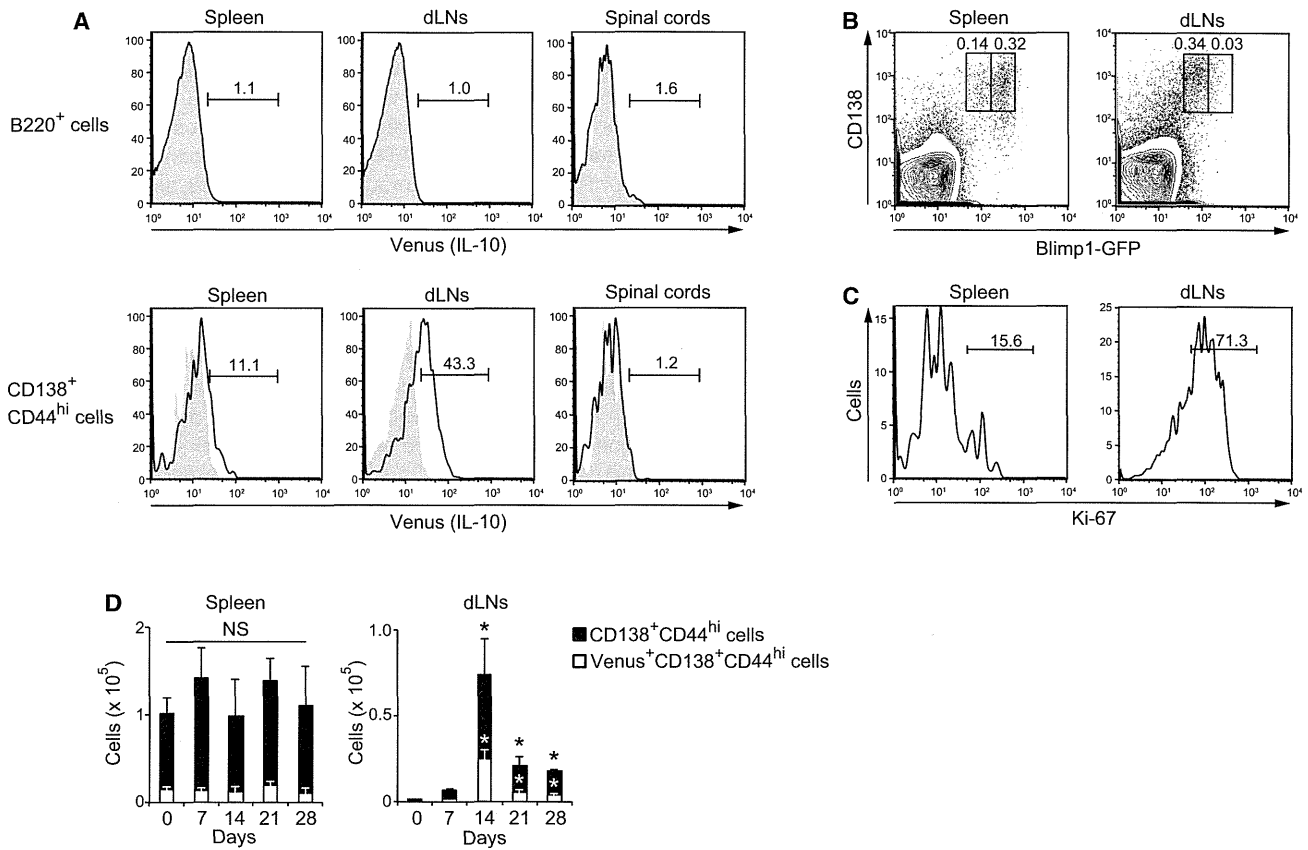


**Figure 1. Plasmablasts Are the Dominant IL-10-Producing B Lineage Cells during EAE**

(A) Flow cytometry of Venus expression in B220<sup>+</sup> and CD138<sup>+</sup>CD44<sup>hi</sup> cells harvested from spleen, dLNs, and spinal cords of wild-type (shaded histogram) and *Il10*<sup>Venus/+</sup> (open histogram) mice 14 days after MOG<sub>35-55</sub> immunization. Percentages of Venus<sup>+</sup> B cells are shown. (B) Flow cytometry of cells from spleen and dLNs of *Prdm1*<sup>GFP/+</sup> mice 14 days after MOG<sub>35-55</sub> immunization. GFP<sup>int</sup> and GFP<sup>hi</sup> populations of CD138<sup>+</sup> cells are gated and their percentages are shown. (C) Flow cytometry of CD138<sup>+</sup>CD44<sup>hi</sup> cells from spleen and dLNs of wild-type mice 14 days after MOG<sub>35-55</sub> immunization. Percentages of Ki-67<sup>+</sup> cells are shown. Data are representative of at least three independent experiments in (A)–(C). (D) Absolute number of CD138<sup>+</sup>CD44<sup>hi</sup> or their Venus<sup>+</sup> cells from spleen and dLNs of *Il10*<sup>Venus/+</sup> mice before and 7, 14, 21, and 28 days after MOG<sub>35-55</sub> immunization. Data are representative of two independent experiments. Data are presented as mean ± SEM for four mice. NS, not significant. \*p < 0.05 versus day 0 (Welch's t test). See also Figure S1.

approaches, we show that plasmablasts in the dLNs were critical for limiting EAE progression. In addition, IL-10 production by plasmablasts requires IRF4 and can prevent dendritic cells from generating pathogenic T cells. Furthermore, human plasmablasts also preferentially secrete IL-10, further highlighting plasmablasts as the IL-10-producing regulatory B cells.

**RESULTS**

**Plasmablasts Are the Main IL-10-Producing B Cells during EAE**

To identify in vivo IL-10-producing B cells and their distribution during autoimmune disease, we elicited EAE in mice carrying a transgene of *Venus*, a variant of yellow fluorescent protein (*Il10*<sup>Venus/+</sup>), which allows tracking of IL-10<sup>+</sup> cells (Atarashi et al., 2011). Although previous reports suggested that several splenic B cell subsets can produce IL-10 (Mauri and Bosma,

2012; Yanaba et al., 2008), we observed little Venus expression in B220<sup>+</sup> B cells before and 14 days after immunization with myelin oligodendrocyte glycoprotein peptide (MOG<sub>35-55</sub>) (Figure 1A and Figures S1A–S1D available online). In contrast, CD138<sup>+</sup>CD44<sup>hi</sup> cells expressed Venus markedly in the dLNs, only modestly in spleen, and not at all in the spinal cords (Figures 1A, S1C, and S1D). ELISA assays also demonstrated that the CD138<sup>+</sup>CD44<sup>hi</sup> population expressing Venus had a potential to produce IL-10 (Figure S1E). CD138<sup>+</sup> cells are composed of highly proliferative plasmablasts and nondividing plasma cells that express intermediate and high amounts of Blimp1 (encoded by the *Prdm1*), respectively (Kallies et al., 2004). By utilizing EAE-induced heterozygous *Prdm1*<sup>GFP/+</sup> knockin mice (*Prdm1*<sup>GFP/+</sup>), we confirmed that CD138<sup>+</sup> cells in spleen and dLNs were largely GFP<sup>hi</sup> plasma cells and GFP<sup>int</sup> plasmablasts, respectively (Figure 1B). CD138<sup>+</sup>CD44<sup>hi</sup> cells in dLNs, but not spleen, were proliferating, as demonstrated by Ki-67 staining

(Figure 1C). Whereas the absolute number of CD138<sup>+</sup>CD44<sup>hi</sup> cells and their Venus<sup>+</sup> cells was essentially constant in spleen, those in dLNs expanded to a peak on day 14 after MOG<sub>35-55</sub> immunization (Figure 1D). Thus, these results indicate that CD138<sup>+</sup> plasmablasts in dLNs are the principal IL-10-producing B lineage cells during EAE.

### Plasmablasts in the dLNs Negatively Regulate EAE Inflammation

A key question is whether IL-10<sup>+</sup>CD138<sup>+</sup> cells are functionally competent to inhibit EAE. To directly address this issue, we elicited EAE in mice conditionally lacking Blimp1 in B lineage cells by crossing of *Prdm1<sup>fl/fl</sup>* with *Mb1<sup>Cre/+</sup>* mice (called *Prdm1<sup>fl/fl</sup>Mb1<sup>Cre/+</sup>* here). Plasma cell differentiation and antibody responses were impaired in these mice (Figures S2A and S2B). EAE development in *Prdm1<sup>fl/fl</sup>Mb1<sup>Cre/+</sup>* mice was greatly exacerbated as compared to *Mb1<sup>Cre/+</sup>* control mice (Figure 2A). Consistent with the exacerbated EAE, CD4<sup>+</sup> T cells, particularly those producing interferon- $\gamma$  (IFN- $\gamma$ ) (Th1 cells) and IL-17 (Th17 cells), increased in the spinal cords of *Prdm1<sup>fl/fl</sup>Mb1<sup>Cre/+</sup>* mice (Figure 2B). When stimulated with MOG<sub>35-55</sub>, *Prdm1<sup>fl/fl</sup>Mb1<sup>Cre/+</sup>* LN cells produced more IFN- $\gamma$  and IL-17 than *Mb1<sup>Cre/+</sup>* cells (Figure 2C). Thus, we conclude that CD138<sup>+</sup> plasmablasts/plasma cells limit EAE inflammation.

Given that IL-10-producing CD138<sup>+</sup> cells are detected in both spleen and dLNs during EAE, it remained important to test which secondary lymphoid organ is critical for EAE attenuation. L-selectin (CD62L), also known as Sell, is an essential homing receptor that governs migration into the peripheral LNs. To explore the involvement of LN B cells in EAE suppression, we generated mixed bone marrow (BM) chimeras by transferring a mixture of BM cells from  $\mu$ MT (80%) and *Sell<sup>-/-</sup>* (20%) mice into lethally irradiated wild-type mice. The *Sell* deficiency was restricted to B cells in the resultant BM chimera (*B-Sell<sup>-/-</sup>*) mice. These mice lacked B lineage cells in LNs, but not spleen, and exhibited increased disease severity compared with control mice (Figure 2D). In striking contrast, mice that had splenectomy developed EAE normally (Figure 2E). B cell population and plasmablast differentiation in the dLNs was not affected by splenectomy. Collectively, these data suggest that plasmablasts in the dLNs negatively regulate EAE, but that splenic B lineage cells are dispensable for its suppression.

Nevertheless, published studies have claimed a functionally important role of splenic B cells to reduce EAE in adoptive transfer experiments (Fillatreau et al., 2002; Matsushita et al., 2008). Based on our above findings, we reasoned that adoptively transferred splenic B cells might give rise to plasmablasts in the dLNs that then regulate EAE. We therefore examined EAE in  $\mu$ MT mice with adoptively transferred splenic B cells isolated from *Prdm1<sup>fl/fl</sup>Mb1<sup>Cre/+</sup>* or *Sell<sup>-/-</sup>* mice and control mice. Although the mice that received B cells from control mice resolved EAE symptoms, these suppressive effects were not observed when *Prdm1<sup>fl/fl</sup>Mb1<sup>Cre/+</sup>* and *Sell<sup>-/-</sup>* B cells were transferred (Figures 2F and 2H). As expected, plasmablast differentiation from control B cells, but not *Prdm1<sup>fl/fl</sup>Mb1<sup>Cre/+</sup>* and *Sell<sup>-/-</sup>* B cells, occurred in LNs (Figures 2G and 2I). These results suggest that splenic B cells can suppress EAE in an adoptive transfer setting but that their plasmablast differentiation in the dLNs might be required.

### EAE Induces Generation of GC-Independent Plasmablasts that Produce IL-10 Preferentially

To gain insight into cellular aspects of IL-10-producing plasmablasts in the dLNs, we first investigated the cell surface phenotype. Most LN plasmablasts in EAE mice expressed high amounts of CD43, CXCR4, and major histocompatibility complex II (MHCII) and low amounts of B220, CD38, and CXCR5 (Figure 3A). Many of them also had undergone immunoglobulin (Ig) class-switch recombination (Figure 3B), which commonly occurs in both extrafollicular and germinal center (GC) responses (Klein and Dalla-Favera, 2008). Because an extensive expansion of GC B cells in the dLNs was detected during EAE (Figure 3C), we investigated the involvement of GCs in regulatory plasmablast generation. We elicited EAE in mice in which the transcription factor *Bcl6* was functionally disrupted by inserting a YFP gene in both of the *Bcl6* alleles (*Bcl6<sup>Yfp/Yfp</sup>*) (Kitano et al., 2011) and found that *Bcl6<sup>Yfp/Yfp</sup>* mice exhibited normal EAE despite of their lack of GC B cells (Figures 3D and 3E). The plasmablast generation was not significantly influenced by loss of *Bcl6* (Figure 3E). Thus, EAE attenuation does not necessarily require GC responses.

We next assessed the potential contribution of anti-inflammatory cytokines besides IL-10 in plasmablasts. Because published studies have suggested that splenic B cells or plasma cells secrete IL-4, IL-13, IL-35, and transforming growth factor- $\beta$  (TGF- $\beta$ ) (Mauri, 2010; Shen et al., 2014), we examined their expression in plasmablasts by quantitative RT-PCR analysis. In agreement with our data obtained with IL-10 reporter mice, CD138<sup>+</sup>CD44<sup>hi</sup> plasmablasts, but not CD19<sup>+</sup>CD138<sup>-</sup> B cells, highly expressed IL-10 (Figure 3F). By contrast, the amount of *Il4*, *Il13*, *Il27* (*Il27b/p28*), *Il35* (*Il12a/Il27b*), and *Tgfb1* mRNA in CD138<sup>+</sup>CD44<sup>hi</sup> cells was decreased or comparable to that in CD19<sup>+</sup> cells. Consistent with that, ELISA and Bio-Plex suspension assay demonstrated preferential IL-10 secretion by CD138<sup>+</sup>CD44<sup>hi</sup> cells (Figure 3G). Although IL-6 and IFN- $\gamma$  produced by B cells have been reported to contribute to EAE pathogenesis (Barr et al., 2012; Matsushita et al., 2006), CD138<sup>+</sup>CD44<sup>hi</sup> cells had little expression of their mRNA and proteins. Collectively, EAE-induced plasmablasts in the dLNs predominantly produce IL-10.

### IRF4 Is Essential for Plasmablast IL-10 Production

We next investigated the mechanisms by which plasmablasts produce IL-10. In a previous study, we found that B cells could secrete IL-10 after BCR stimulation in a Ca<sup>2+</sup> influx-dependent way (Matsumoto et al., 2011). However, this occurred only when B cells were preactivated with TLR agonists. Thus, we reasoned that TLR-dependent transcription factors would be required for plasmablast differentiation and/or IL-10 production. To this end, LPS-stimulated B cells from *Prdm1<sup>9fp/+</sup>* mice were sorted on the basis of GFP and CD138 expression followed by stimulation with anti-IgM (Figure 4A). IL-10 secretion was restricted to GFP<sup>+</sup> fractions and drastically enhanced by BCR ligation (Figure 4B). Because both CD138<sup>+</sup>GFP<sup>+</sup> and CD138<sup>-</sup>GFP<sup>+</sup> populations are known to have characteristics of antibody secretion and proliferative responses (Kallies et al., 2004), we concluded that plasmablasts are the principal IL-10 producers in vitro. Unexpectedly, however, B cells lacking Blimp1 proteins secreted IL-10 normally despite having impaired CD138<sup>+</sup>

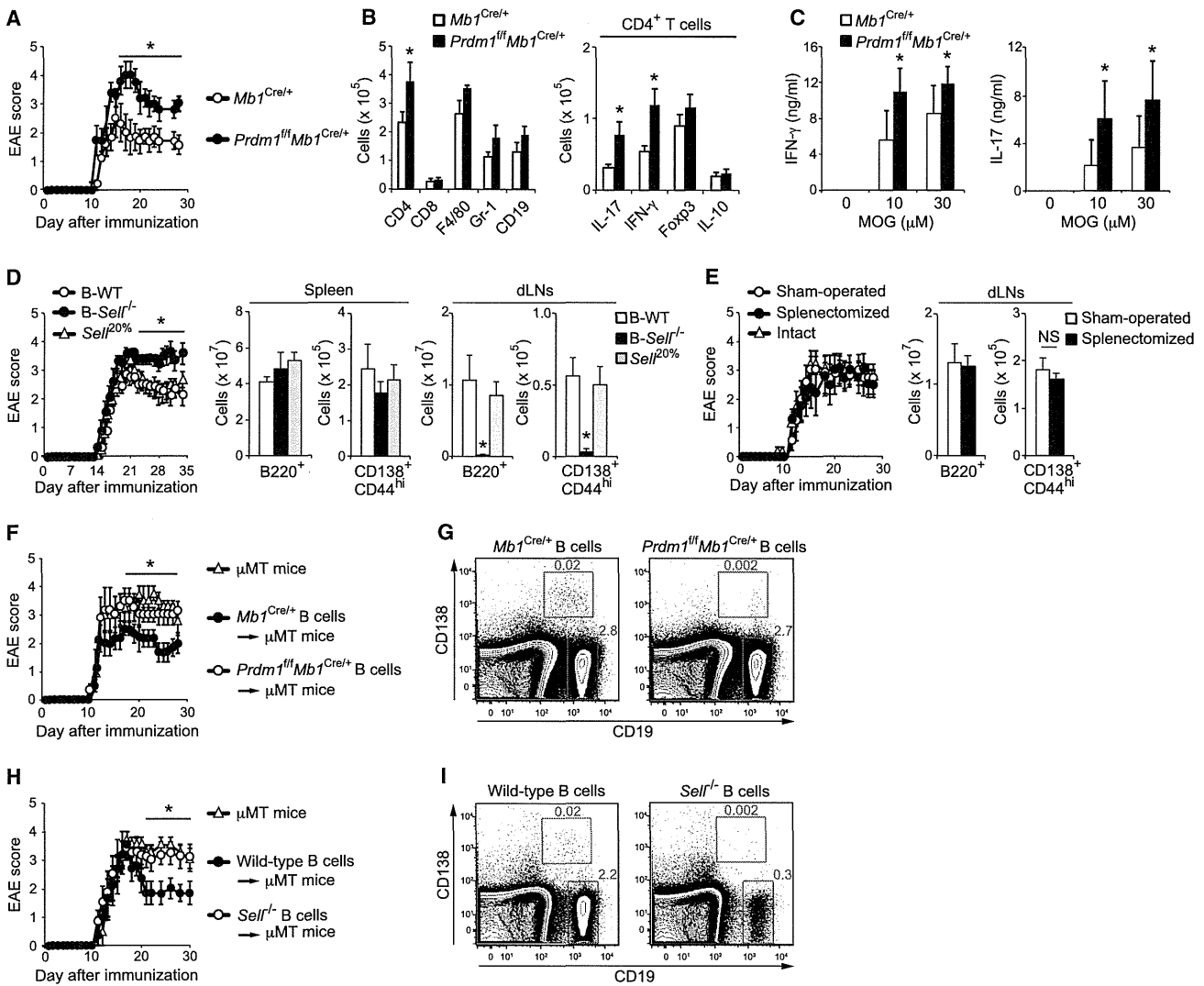


**Figure 2. Plasmablasts in the dLNs Negatively Regulate EAE Inflammation**

(A) Clinical EAE scores for *Mb1<sup>Cre/+</sup>* and *Prdm1<sup>fl/fl</sup>Mb1<sup>Cre/+</sup>* mice immunized with MOG<sub>35-55</sub>. The EAE score is shown as mean ± SEM for six to seven mice.  
 (B) Absolute number of cells from spinal cords harvested from *Mb1<sup>Cre/+</sup>* and *Prdm1<sup>fl/fl</sup>Mb1<sup>Cre/+</sup>* mice 14 days after MOG<sub>35-55</sub> immunization. Data are presented as mean ± SEM for five mice.  
 (C) ELISA of IFN-γ and IL-17 by cells isolated from the dLNs of *Mb1<sup>Cre/+</sup>* and *Prdm1<sup>fl/fl</sup>Mb1<sup>Cre/+</sup>* mice 14 days after EAE induction followed by stimulation with MOG<sub>35-55</sub> for 48 hr. Data are presented as mean ± SD.  
 (A–C) \*p < 0.05 versus *Mb1<sup>Cre/+</sup>* mice (Mann-Whitney U test).  
 (D) Clinical EAE scores for B-*Sell<sup>-/-</sup>* (chimeric mice generated by transplanting a mixture of BM cells from μMT (80%) and *Sell<sup>-/-</sup>* (20%) mice and two control chimera groups: wild-type mice lethally irradiated and reconstituted with 80% μMT plus 20% wild-type bone marrow (B-WT) or reconstituted with 80% wild-type plus 20% *Sell<sup>-/-</sup>* bone marrow (*Sell<sup>20%</sup>*). The absolute number of B220<sup>+</sup> and CD138<sup>+</sup>CD44<sup>hi</sup> cells harvested from spleen and dLNs of chimeras 14 days after MOG<sub>35-55</sub> immunization is shown on the right. Data are shown as mean ± SEM for five to ten mice. \*p < 0.05 versus B-WT mice (Mann-Whitney U test).  
 (E) Clinical EAE scores for sham-operated, splenectomized, and intact wild-type mice immunized with MOG<sub>35-55</sub>. Absolute number of B220<sup>+</sup> and CD138<sup>+</sup>CD44<sup>hi</sup> cells from dLNs of sham-operated and splenectomized mice 14 days after MOG<sub>35-55</sub> immunization is shown on the right. Data are shown as mean ± SEM for five to seven mice. NS, not significant (Mann-Whitney U test).  
 (F) Clinical EAE scores for μMT mice immunized with MOG<sub>35-55</sub> after injecting splenic B cells harvested from *Mb1<sup>Cre/+</sup>* and *Prdm1<sup>fl/fl</sup>Mb1<sup>Cre/+</sup>* mice 28 days after EAE induction. The EAE score is shown as mean ± SEM for five to six mice. \*p < 0.05 versus *Prdm1<sup>fl/fl</sup>Mb1<sup>Cre/+</sup>* B cells (Mann-Whitney U test).  
 (G) Flow cytometry of cells from dLNs of μMT mice immunized for 12 days with MOG<sub>35-55</sub> after injecting splenic *Mb1<sup>Cre/+</sup>* and *Prdm1<sup>fl/fl</sup>Mb1<sup>Cre/+</sup>* B cells.  
 (H) Clinical EAE scores for μMT mice immunized with MOG<sub>35-55</sub> after injecting splenic B cells harvested from wild-type and *Sell<sup>-/-</sup>* mice. The EAE score is shown as mean ± SEM for five to nine mice. \*p < 0.05 versus *Sell<sup>-/-</sup>* B cells (Mann-Whitney U test).  
 (I) Flow cytometry of cells from dLNs of μMT mice immunized for 12 days with MOG<sub>35-55</sub> after injecting splenic wild-type and *Sell<sup>-/-</sup>* B cells. CD19<sup>+</sup> and CD138<sup>+</sup> cells are gated and their percentages are shown (G and I).  
 Data are representative from three (A–D and F) or two (E and G–I) independent experiments. See also Figure S2.



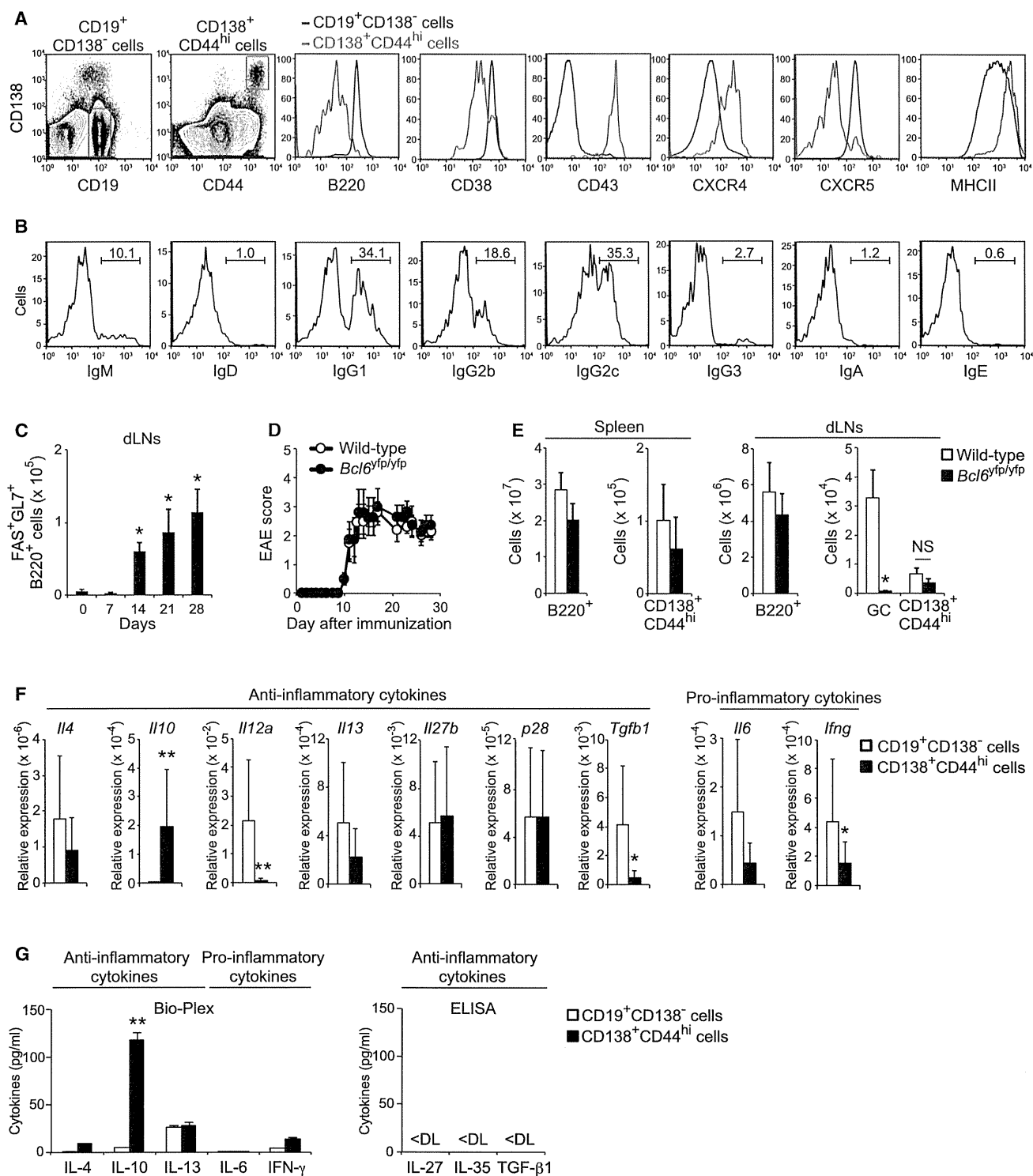


**Figure 3. EAE Induces Generation of GC-Independent Plasmablasts that Produce IL-10 Preferentially**

(A) Flow cytometry of CD19<sup>+</sup>CD138<sup>-</sup> (black histogram, gated as in the left-most panel) and CD138<sup>+</sup>CD44<sup>hi</sup> cells (red histogram, gated as in second panel from the left) harvested from dLNs of wild-type mice 14 days after MOG<sub>35-55</sub> immunization.

(B) Flow cytometry of CD138<sup>+</sup>CD44<sup>hi</sup> cells harvested from dLNs of wild-type mice 14 days after MOG<sub>35-55</sub> immunization. Percentages of Ig<sup>+</sup> cells are shown.

(C) Absolute number of FAS<sup>+</sup>GL7<sup>+</sup>B220<sup>+</sup> (GC) B cells from dLNs harvested from wild-type mice before and 7, 14, 21, and 28 days after MOG<sub>35-55</sub> immunization. Data are presented as mean  $\pm$  SEM for five to six mice. \*p < 0.05 versus day 0 (Mann-Whitney U test).

(D) Clinical EAE scores for wild-type and *Bcl6*<sup>yp/yp</sup> mice immunized with MOG<sub>35-55</sub>. The EAE score is shown as mean  $\pm$  SEM for seven mice.

(legend continued on next page)

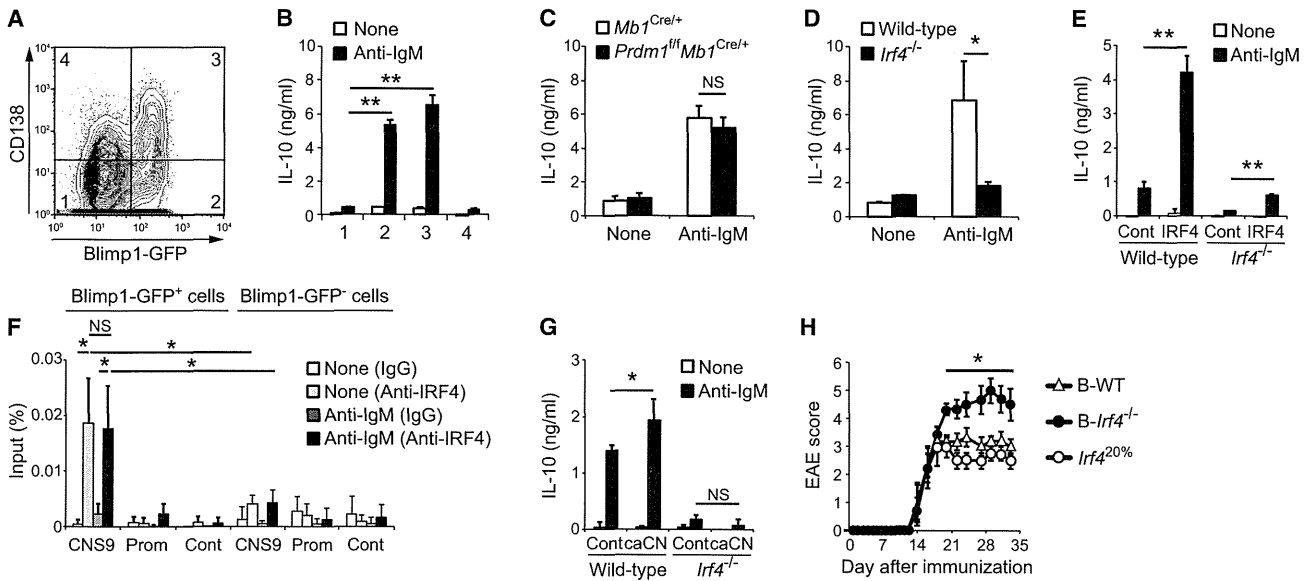


**Figure 4. IRF4 Is Essential for Plasmablast IL-10 Production**

(A) Flow cytometry of B cells isolated from spleen of *Prdm1<sup>GFP/+</sup>* mice and cultured with LPS for 48 hr. Four populations—GFP<sup>-</sup>CD138<sup>-</sup> (fraction 1), GFP<sup>+</sup>CD138<sup>-</sup> (fraction 2), GFP<sup>+</sup>CD138<sup>+</sup> (fraction 3), and GFP<sup>-</sup>CD138<sup>+</sup> (fraction 4) cells—were sorted and assayed in (B). (B) ELISA of IL-10 secreted by the sorted B cells after stimulation with anti-IgM for 24 hr. (C) ELISA of IL-10 secreted by B cells isolated from peripheral LNs of *Mb1<sup>Cre/+</sup>* and *Prdm1<sup>fl/fl</sup>Mb1<sup>Cre/+</sup>* mice and cultured with LPS for 48 hr followed by stimulation with anti-IgM for 24 hr. (D) ELISA of IL-10 secreted by B cells isolated from peripheral LNs of wild-type and *Irf4<sup>-/-</sup>* mice and cultured with LPS for 48 hr followed by stimulation with anti-IgM for 24 hr. (E) ELISA of IL-10 secreted by GFP<sup>+</sup> cells sorted from LPS-activated wild-type and *Irf4<sup>-/-</sup>* B cells retrovirally transduced with GFP alone (Cont) or IRF4 followed by stimulation with anti-IgM for 24 hr. (F) ChIP analysis of GFP<sup>+</sup> plasmablasts and GFP<sup>-</sup> B cells sorted from LPS-activated *Prdm1<sup>GFP/+</sup>* B cells, stimulated with anti-IgM for 30 min, and then precipitated with anti-IRF4 Ab or goat IgG. Input DNA and precipitated DNA were quantified by RT-PCR with PCR primers specific for CNS9 and promoter (Prom) regions of *Ii10* or 3' region of *Cd19* (Cont). Data shown are pooled from two independent experiments. (G) ELISA of IL-10 secreted by GFP<sup>+</sup> cells sorted from LPS-activated wild-type and *Irf4<sup>-/-</sup>* B cells retrovirally transduced with GFP alone (Cont) or constitutively active calcineurin (caCN) followed by stimulation with anti-IgM for 24 hr. NS, not significant. (H) Clinical EAE scores for chimeric mice in which only B cells lacked IRF4 (*B-Irf4<sup>-/-</sup>*; wild-type mice lethally irradiated and reconstituted with 80%  $\mu$ MT plus 20% *Irf4<sup>-/-</sup>* bone marrow) and two control chimera groups: wild-type mice lethally irradiated and reconstituted with 80%  $\mu$ MT plus 20% wild-type bone marrow (B-WT) or reconstituted with 80% wild-type plus 20% *Irf4<sup>-/-</sup>* bone marrow (*Irf4<sup>20%</sup>*). The EAE score is shown as mean  $\pm$  SEM for five to six mice. \**p* < 0.05 versus B-WT mice (Mann-Whitney U test). (B–G) Data are presented as mean  $\pm$  SD. \**p* < 0.05, \*\**p* < 0.001 (Student's *t* test). Data are representative of three (A–E and G) or two (H) independent experiments. See also Figures S3 and S4.

cell generation (Figures 4C, S3A, and S3B), suggesting that Blimp1 in developing plasmablasts is dispensable for IL-10 production. Importantly, B cells lacking Blimp1 fail to fully differentiate into plasma cells, but rather initiate this differentiation pathway (Kallies et al., 2007; Kallies and Nutt, 2007; Shapiro-Shelef et al., 2003). Therefore, we next focused on the functional importance of IRF4 because it is a critical factor in the early phase of plasma cell differentiation and one of the downstream targets of TLR and BCR signaling (Mittrücker et al., 1997; Oracki et al., 2010). LPS-activated *Irf4<sup>-/-</sup>* B cells had impaired IL-10 secretion

after BCR ligation (Figure 4D). Reciprocally, retroviral expression of IRF4 in wild-type B cells substantially increased IL-10 production and partially rescued it in *Irf4<sup>-/-</sup>* B cells (Figure 4E). Furthermore, chromatin immunoprecipitation (ChIP) analysis revealed that IRF4 in plasmablasts bound to the *Ii10* CNS9 region, which controls *Ii10* expression and is located approximately 9.1 kbp upstream of the transcription start site (Lee et al., 2009), though this binding frequency was unaffected by BCR stimulation (Figure 4F). These results imply that IRF4 not only induces plasmablast generation but also directly regulates *Ii10* expression. Nuclear factor

(E) Absolute number of each B cell subset from spleen and dLNs harvested from wild-type and *Bcl6<sup>Yfp/Yfp</sup>* mice 28 days after MOG<sub>35–55</sub> immunization. Data are presented as mean  $\pm$  SEM for six mice. \**p* < 0.05 versus wild-type mice (Mann-Whitney U test). NS, not significant.

(F and G) Quantitative RT-PCR (F) and ELISA and Bio-Plex cytokine (G) analysis of CD19<sup>+</sup>CD138<sup>-</sup> and CD138<sup>+</sup>CD44<sup>hi</sup> cells harvested from dLNs of wild-type mice 14 days after MOG<sub>35–55</sub> immunization. For ELISA and Bio-Plex suspension assay, the isolated CD19<sup>+</sup>CD138<sup>-</sup> and CD138<sup>+</sup>CD44<sup>hi</sup> cells were stimulated with PMA and ionomycin for 5 hr (G). Data are presented as mean  $\pm$  SD. Abbreviations: <DL, below detection limit. \**p* < 0.05, \*\**p* < 0.001 versus CD19<sup>+</sup> cells (Student's *t* test).

Data are representative from three (A, B, and F) or two (C–E and G) independent experiments.

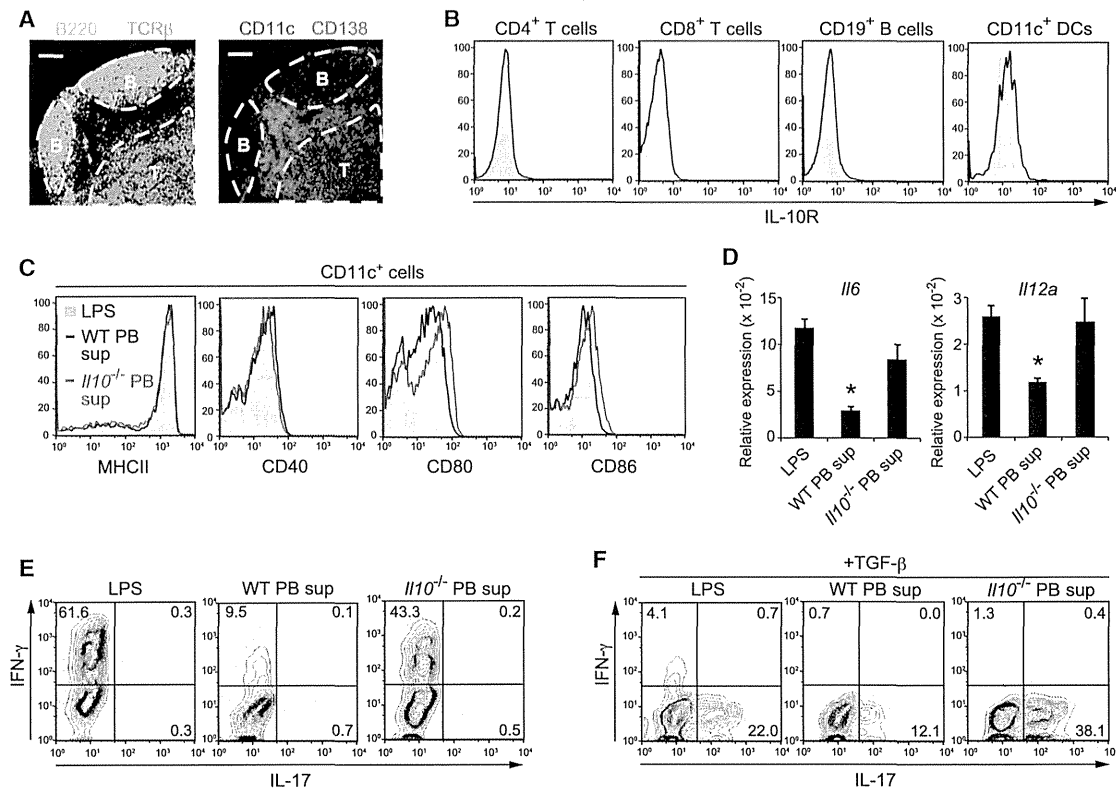


**Figure 5. Plasmablasts Inhibit Dendritic Cell Function to Generate Autoreactive T Cells**

(A) Histological analysis of dLNs harvested from wild-type mice 14 days after MOG<sub>35-55</sub> immunization. Sections were stained with B220 and TCR- $\beta$  Abs (left) or with CD11c and CD138 Abs (right). Original magnification,  $\times 10$ ; scale bars represent 100  $\mu$ m.

(B) Flow cytometry of IL-10R expression by cells harvested from dLNs of wild-type mice 14 days after MOG<sub>35-55</sub> immunization. Cells were stained with an IL-10R mAb (open histogram) or isotype control (shaded histogram).

(C) Flow cytometry of CD11c<sup>+</sup> cells harvested from dLNs of wild-type mice 14 days after MOG<sub>35-55</sub> immunization followed by stimulation with LPS alone (shaded histogram) or supernatants from wild-type plasmablasts (PB) (WT PB sup; black histogram) and *Il10*<sup>-/-</sup> plasmablasts (*Il10*<sup>-/-</sup> PB sup; red histogram) activated with LPS and then anti-IgM.

(D) Quantitative RT-PCR analysis of *Il6* and *Il12a* transcripts in CD11c<sup>+</sup> cells harvested from dLNs of wild-type mice 14 days after MOG<sub>35-55</sub> immunization, stimulated with LPS or WT and *Il10*<sup>-/-</sup> PB sup, normalized to the expression of *Gapdh*. Data are presented as mean  $\pm$  SD. \* $p < 0.05$  versus DC treated with *Il10*<sup>-/-</sup> PB sup (Student's *t* test).

(E and F) Cytokine profiles of TCR<sup>MOG</sup>-expressing naive CD4<sup>+</sup> T cells cocultured with dLN CD11c<sup>+</sup> cells stimulated with LPS or WT and *Il10*<sup>-/-</sup> PB sup in the absence (E) or presence (F) of TGF- $\beta$  together with MOG<sub>35-55</sub> for 72 hr. Percentages of IFN- $\gamma$ <sup>+</sup> and/or IL-17<sup>+</sup> cells are shown.

Results represent one of three similar experiments. See also Figure S5.

of activated T cells (NFAT), which is activated by Ca<sup>2+</sup> and the calmodulin-dependent phosphatase calcineurin, is also vital for BCR-induced IL-10 production (Matsumoto et al., 2011). Retroviral expression of a constitutively active form of calcineurin A (caCN) markedly increased BCR-induced IL-10 production in an IRF4-dependent manner (Figure 4G), suggesting that NFAT-dependent IL-10 production requires IRF4. Moreover, we found that IRF4 has a B cell regulatory role in vivo because B-cell-specific *Irf4*-deficient chimeric mice lacking CD138<sup>+</sup>CD44<sup>hi</sup> cells in the dLNs became susceptible to EAE (Figures 4H and S4). Together, these data indicate that IRF4 is essential for B cell IL-10 production to suppress EAE.

#### Plasmablast-Derived IL-10 Inhibits Dendritic Cell Function to Generate Pathogenic T Cells

We next elucidated the mechanisms by which plasmablasts suppress EAE. Immunohistochemical analysis of the dLNs in

EAE-induced mice revealed that CD138<sup>+</sup> plasmablasts were mainly colocalized with CD11c<sup>+</sup> dendritic cells (DCs) in the extra-follicular region between T cell zones and B cell follicles (Figure 5A). Given that DCs, but not T and B cells, expressed detectable amounts of IL-10 receptor (IL-10R) (Figure 5B), we next examined whether DC function is affected by plasmablast-derived IL-10. When DCs were stimulated with supernatants derived from wild-type plasmablasts activated with LPS and then anti-IgM, the expression of MHCII, CD40, CD80, and CD86 was unchanged, but *Il6* and *Il12* mRNA was significantly decreased. This effect was not observed with *Il10*<sup>-/-</sup> plasmablasts (Figures 5C and 5D). Consistent with these results, Th1 cell differentiation of MOG-specific T cells was markedly prevented by supernatants from wild-type, but not *Il10*<sup>-/-</sup>, plasmablasts when cocultured with DCs (Figure 5E). Very similar results were obtained with TGF- $\beta$ -mediated Th17 cell generation (Figure 5F). Furthermore, we also observed equivalent results

when DCs were cocultured with Blimp1-GFP<sup>+</sup> plasmablasts (Figure S5). Thus, these results suggest that IL-10-producing plasmablasts inhibit DC functions to generate autoreactive T cells. This does not exclude the possibility that other cell types will be affected in vivo by plasmablast IL-10.

### Human Plasmablasts Are IL-10-Producing B Cells

Our findings that plasmablasts represent the IL-10-producing B cells in mice led us to test whether this also applies to humans. B cells were isolated from peripheral blood of healthy donors and cultured with CpG (a TLR9 agonist) and/or cytokine cocktails including IL-2, IL-6, and interferon-alpha (IFN- $\alpha$ ), which are known to provide conditions for effective plasmablast differentiation (Jego et al., 2003; Joo et al., 2012). Indeed, we detected CD27<sup>hi</sup>CD38<sup>+</sup> putative plasmablasts after culture with CpG, while concomitant treatment with CpG and cytokine cocktails induced a greater frequency of an additional population of CD27<sup>int</sup>CD38<sup>+</sup> cells as well as CD27<sup>int</sup>CD38<sup>+</sup> cells (Figure 6A). In particular, IFN- $\alpha$  was considerably effective for CD27<sup>int</sup>CD38<sup>+</sup> differentiation and essentially the same results were obtained with IFN- $\beta$  instead of IFN- $\alpha$  (Figure S6A). We found that IL-10 production was greatly induced in culture with a mixture of CpG and cytokine cocktails (Figure 6B). Both CD27<sup>hi</sup>CD38<sup>+</sup> and CD27<sup>int</sup>CD38<sup>+</sup> populations had a progressive loss of CD20, CD180, and Pax5 (Figures 6C, S6B, and S6C). Inversely, they had higher expression of IRF4, Blimp1, and XBP1 proteins and their transcripts (Figures 6C and S6C) and showed morphological maturation into plasma cells, as displayed by larger size with abundant cytoplasm, eccentric nuclei, and perinuclear haloes (Figure 6D). Consistent with these observations, both CD27<sup>hi</sup>CD38<sup>+</sup> and CD27<sup>int</sup>CD38<sup>+</sup> cells substantially secreted IgM (Figure 6E). Given the lack of a human mature plasma cell marker CD138 (Figure S6B), CD27<sup>int</sup>CD38<sup>+</sup> cells as well as CD27<sup>hi</sup>CD38<sup>+</sup> cells can be considered as plasmablasts whereas the CD27<sup>hi</sup> cells apparently are more mature than CD27<sup>int</sup> cells in view of their phenotypes. To determine which populations produce IL-10, we purified four fractions based on CD27 and CD38 expression after culture. ELISA assay showed that CD27<sup>int</sup>CD38<sup>+</sup> plasmablasts selectively secreted IL-10 (Figure 6F). As a further test of this finding, we conducted IL-10 secretion assay by using IL-10 capture and detection antibodies, which allow us to detect live IL-10-secreting cells and found that the majority of IL-10<sup>+</sup> B cells consisted of CD27<sup>int</sup>CD38<sup>+</sup> cell fraction (Figure 6G). Of note, this IL-10<sup>+</sup>CD27<sup>int</sup>CD38<sup>+</sup> population substantially secreted IgM, as assessed by ELISPOT assay (Figure 6H), suggesting that IL-10-producing B cells are Ig-secreting CD27<sup>int</sup>CD38<sup>+</sup> plasmablasts.

We next addressed the issue of why CD27<sup>int</sup>, but not CD27<sup>hi</sup>, plasmablasts produce IL-10. Given that freshly prepared peripheral blood B cells consist of three major populations, i.e., CD24<sup>lo</sup>CD27<sup>-</sup>CD38<sup>-</sup> (naive mature), CD24<sup>hi</sup>CD27<sup>-</sup>CD38<sup>lo</sup> (naive immature), and CD24<sup>hi</sup>CD27<sup>+</sup>CD38<sup>-</sup> (memory) cells (Figure 6I), the origin of each might be different. To test this hypothesis, they were sorted and then cultured. Memory B cells were predominantly differentiated into CD27<sup>hi</sup>CD38<sup>+</sup> plasmablasts, whereas naive immature B cells and mature B cells, albeit to a lesser degree, became CD27<sup>int</sup>CD38<sup>+</sup> plasmablasts (Figure 6I). Naive B-cell-derived CD27<sup>int</sup> plasmablasts produced considerably more IL-10 (Figures 6J, S6D, and S6E). Collectively, these

findings establish that human plasmablasts that arise from naive and especially immature B cells, but not memory B cells, are the major IL-10-producing B cells.

### DISCUSSION

Our findings identify plasmablasts as the IL-10-producing B cells that can suppress autoimmunity. This was the case for EAE, where they were developed in the dLNs under the control of Blimp1 and IRF4 and disease progression was enhanced by their deletion. Furthermore, human plasmablasts also preferentially secreted IL-10, and these cells were derived from naive but not memory B cells.

It was previously thought that splenic B cells secrete the IL-10 that limits EAE. Instead, we found that CD138<sup>+</sup> plasmablasts in the dLNs were the major producers of this cytokine during EAE. This was the case when assessed by *I10*<sup>Venus/+</sup> reporter mice or quantitative RT-PCR. In accordance with previous reports using several other IL-10 reporter lines injected with LPS or infected with *Salmonella* (Madan et al., 2009; Maseda et al., 2012; Shen et al., 2014), we also observed Venus expression in splenic CD138<sup>+</sup> cells in *I10*<sup>Venus/+</sup> mice. However, amounts were very low and the frequency of positive cells was unaffected by EAE induction. By contrast, IL-10<sup>+</sup> plasmablasts in the dLNs were newly generated within extrafollicular foci, implying negative feedback regulation to protect excessive inflammation.

Our finding of severe EAE pathogenesis in the absence of plasmablasts due to B-cell-specific deletion of Blimp1 or IRF4 supports the idea that plasmablasts possess regulatory activity in vivo. This regulatory function is dependent on the dLNs and independent of the spleen. On the other hand, results from adoptive transfer studies were interpreted to mean that splenic B cells, especially the CD1d<sup>hi</sup>CD5<sup>+</sup> B cell population, could suppress EAE through some unknown mechanism (Matsushita et al., 2008). Although we also observed that adoptive transfer of splenic B cells normalized EAE, plasmablast generation in the dLNs was required. CD1d<sup>hi</sup>CD5<sup>+</sup> B cells extensively differentiate into plasmablasts in culture (Maseda et al., 2012) and their adoptive transfer from mice lacking IL-21R, CD40, and MHCII, which are indispensable for plasma cell differentiation (McHeyzer-Williams et al., 2012), into *Cd19*<sup>-/-</sup> mice does not resolve EAE development (Yoshizaki et al., 2012). Therefore, this population might serve as plasmablast precursors in an adoptive transfer setting.

The finding of in vitro BCR-dependent IL-10 production specifically in Blimp1<sup>+</sup> cells provides further evidence for the importance of plasmablasts and can explain the previously demonstrated need for TLR signaling for BCR-mediated IL-10 expression (Matsumoto et al., 2011). This idea is also supported by the observation of impaired IL-10 secretion in the absence of IRF4, which resulted in defective plasmablast differentiation (Figure S3A). Thus, IRF4 is required for IL-10 expression along with plasmablast differentiation in vitro and in vivo. Importantly, TLR and BCR signals induce the expression of IRF4 (De Silva et al., 2012) and therefore operate upstream of both plasmablast differentiation and IL-10 production. We detected deposition of IRF4 at the CNS9 region upstream enhancer in the *I10* locus. This is in agreement with published studies that demonstrated

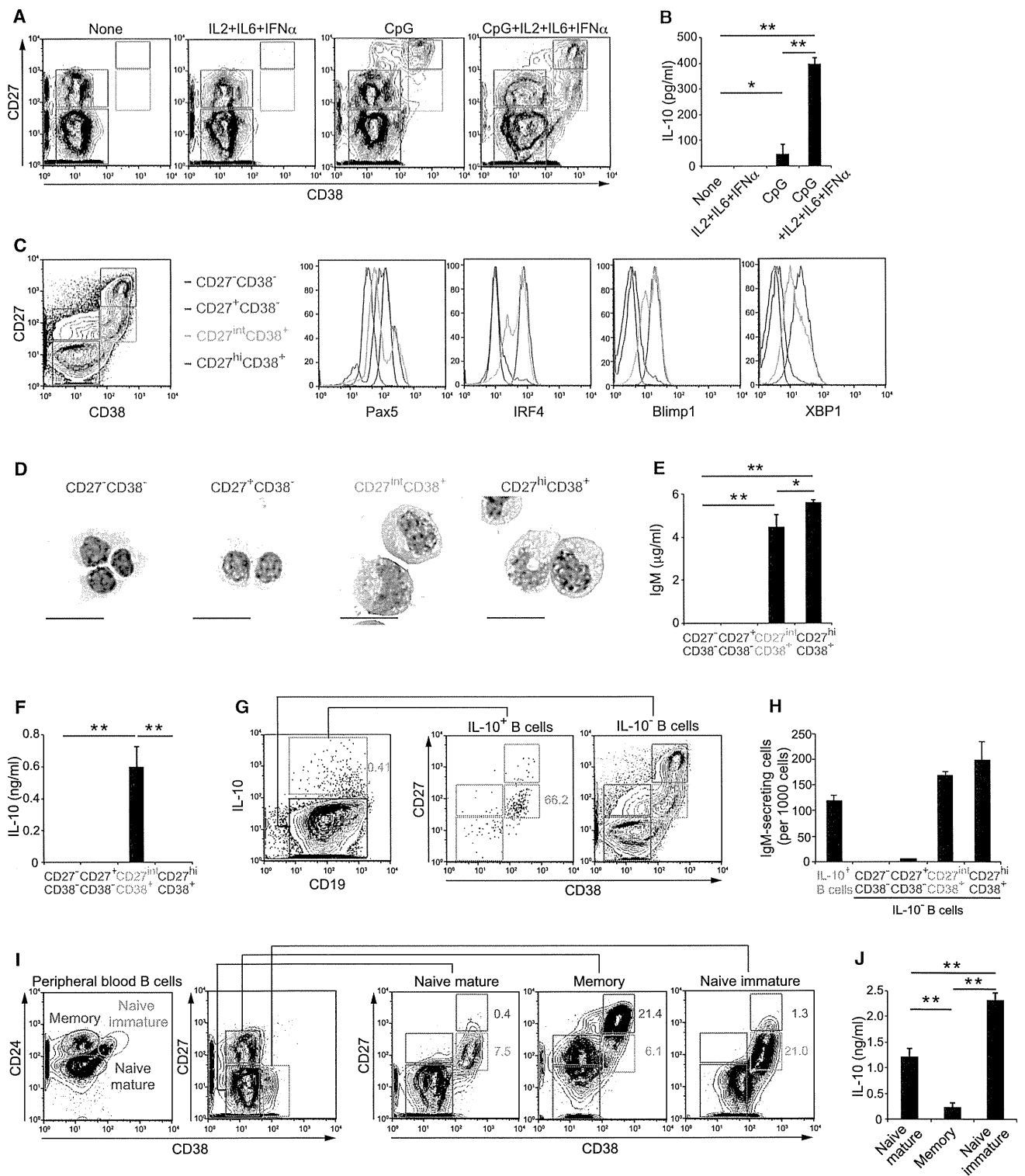


**Figure 6. Human Plasmablasts Are IL-10-Producing B Cells**

(A) Flow cytometry of B cells isolated from healthy blood donors and cultured with IL-2, IL-6 plus IFN- $\alpha$  (IL2, IL6, IFN $\alpha$ ), and/or CpG for 96 hr. Four populations—CD27<sup>-</sup>CD38<sup>-</sup> (red), CD27<sup>+</sup>CD38<sup>-</sup> (blue), CD27<sup>int</sup>CD38<sup>+</sup> (green), and CD27<sup>hi</sup>CD38<sup>+</sup> (purple) cells—are gated.

(B) ELISA of IL-10 secreted by B cells isolated from peripheral blood of healthy donors and cultured with IL-2, IL-6 plus IFN- $\alpha$ , and/or CpG for 96 hr.

(C) Flow cytometry of B cell populations indicated in the left panel.

(legend continued on next page)

IRF4 binding to the same element in various types of cells (Cretney et al., 2011; Lee et al., 2009; Li et al., 2012). NFAT bound to the same region in Th2 cells, which was essential for IL-10 transcription (Lee et al., 2009). Taking into account our previous finding that B-cell-mediated IL-10 production requires NFAT activation (Matsumoto et al., 2011), it seems likely that IRF4 serves as an NFAT transcription partner to produce IL-10 in plasmablasts.

Unexpectedly, Blimp1-deficient B cells secreted IL-10 in our in vitro experiments despite impaired CD138<sup>+</sup> cell differentiation. Considering that the initiation of plasma cell differentiation takes place in vitro in the absence of Blimp1 (Kallies et al., 2007), it seems possible that IL-10 production is initiated already in the early preplasmablastic stage of plasma cell development, which is independent of Blimp1 (Kallies et al., 2007). However, we could detect little Venus-positive CD138<sup>-</sup> B cell population in mice during EAE (data not shown). Given that GFP<sup>+</sup>CD138<sup>-</sup> cells in *Prdm1<sup>9fp/+</sup>* mice were effectively generated in vitro (Figure 4A), but not in vivo (Figure 1B), it seems likely that no or few preplasmablasts as is detected in culture exist in vivo.

We now have evidence that naive B-cell-derived plasmablasts represent the most significant IL-10 producers in humans. Although activation of human peripheral blood B cells with CpG caused CD27<sup>hi</sup>CD38<sup>+</sup> plasmablast generation, our results establish that additional treatment with cytokines including IL-2, IL-6, and, especially, IFN- $\alpha$  drove the differentiation of CD27<sup>int</sup>CD38<sup>+</sup> plasmablasts that predominantly secrete IL-10. Given that IFN- $\alpha$  enhances CD38<sup>+</sup> expression on naive B cells (Giordani et al., 2009) and can induce plasma cell differentiation (Jego et al., 2003), IFN receptor signals seem likely to be key for IL-10-producing plasmablast generation. Indeed, patients with SLE have high serum IFN- $\alpha$  concentrations (Kim et al., 1987) and increased CD27<sup>int</sup>CD38<sup>+</sup> cells in peripheral blood (Arce et al., 2001), suggesting that IL-10<sup>+</sup> plasmablast expansion might be the result of the inflammatory conditions. Furthermore, the treatment with IFN- $\beta$ , another type I IFN approved for MS therapy, enhances B cell IL-10 secretion after BCR and CD40 ligation (Ramgolam et al., 2011). Although the precise mechanism by which IFN- $\beta$  suppresses MS remains unclear, one of the possible explanations is that IFN- $\beta$  might promote generation of IL-10-producing plasmablasts. Noteworthy, in clinical trials, MS patients who received Atacicept, a transmembrane activator and calcium-modulating cyclophilin-ligand interactor (TACI)-Ig fusion protein to deplete anti-

body-secreting cells, had exacerbated inflammatory symptoms (Hartung and Kieseier, 2010). This would be consistent with an inhibitory function for human plasmablasts. We have provided evidence that IL-10-producing plasmablasts effectively stem from naive immature B cells. This might support a recent study that human IL-10-competent B cells were enriched in immature CD24<sup>hi</sup>CD38<sup>hi</sup> B cells after culture with CD40 stimulation (Blair et al., 2010). We found that memory B-cell-derived plasmablasts failed to secrete IL-10, suggesting that the immediate precursor of developing plasmablasts would dictate the balance between cells that promote autoimmunity by antibody production or have regulatory capacity that protects from overt pathology.

In conclusion, our findings have identified plasmablasts in the dLNs as the IL-10-producing B cells that suppress autoimmunity. We also established a phenotype for human plasmablasts that predominantly secreted IL-10. Our study might lead to better understanding of the nature of autoimmune diseases and provide a basis for exploring new therapeutic strategies.

## EXPERIMENTAL PROCEDURES

### Mice

C57BL/6 mice were purchased from CLEA Japan. *Bcl6<sup>9fp/9fp</sup>* (Kitano et al., 2011), *Il10<sup>Venus/+</sup>* (Atarashi et al., 2011), *Irf4<sup>-/-</sup>* (Mitrücker et al., 1997; Suzuki et al., 2004), *Mb1<sup>Cre/+</sup>* (Hobeika et al., 2006),  $\mu$ MT (Kitamura et al., 1991), and *Prdm1<sup>9fp/+</sup>* (Kallies et al., 2004) mice have been described previously. *Il10<sup>-/-</sup>*, *Prdm1<sup>9fp/+</sup>*, *Sell<sup>-/-</sup>*, and TCR<sup>MOG</sup> transgenic mice were purchased from the Jackson Laboratory. We generated *Prdm1<sup>9fp/+</sup>Mb1<sup>Cre/+</sup>* mice by crossing of *Prdm1<sup>9fp/+</sup>* mice with *Mb1<sup>Cre/+</sup>* mice. Mice were bred and maintained under specific-pathogen-free conditions and used at 6 to 12 weeks of age. Animal care and experiments were conducted according to the guidelines established by the animal committee of Osaka University.

### Generation of Mixed Bone Marrow Chimeras

Mixed bone marrow chimeras were produced as described previously (Fillatreau et al., 2002). In brief, recipient wild-type mice received 800 cGy of X-ray irradiation. One day later, the recipients were reconstituted with a mixed inoculum of 80%  $\mu$ MT bone marrow cells supplemented with 20% bone marrow cells from *Irf4<sup>-/-</sup>* or *Sell<sup>-/-</sup>* mice. Control groups received 80%  $\mu$ MT and 20% wild-type bone marrow cells or 80% wild-type and 20% bone marrow cells from *Irf4<sup>-/-</sup>* or *Sell<sup>-/-</sup>* mice. Chimeric mice were left to fully reconstitute their lymphoid system for at least 12 weeks before EAE induction.

### Induction and Assessment of EAE

EAE was induced by subcutaneous immunization with 200  $\mu$ g of MOG<sub>35-55</sub> (MBL) emulsified in complete Freund's adjuvant (CFA) containing 500  $\mu$ g of

(D) May-Grünwald-Giemsa staining of sorted B cell populations after culture with IL-2, IL-6, IFN- $\alpha$  plus CpG for 96 hr. Original magnification,  $\times$ 400; scale bars represent 20  $\mu$ m.

(E and F) ELISA of IgM (E) and IL-10 (F) secreted by the indicated B cell populations after culture with IL-2, IL-6, IFN- $\alpha$  plus CpG for 96 hr and then cultured for an additional 24 hr.

(G) Flow cytometry of B cells cultured with IL-2, IL-6, IFN- $\alpha$  plus CpG for 96 hr and labeled with IL-10 capture and detection antibodies to detect IL-10<sup>+</sup> B cells. Percentage of IL-10<sup>+</sup> B cells and IL-10<sup>+</sup>CD27<sup>int</sup>CD38<sup>+</sup> cells are shown.

(H) ELISPOT of IgM secreted by the indicated B cell populations after culture with IL-2, IL-6, IFN- $\alpha$  plus CpG for 96 hr followed by an additional 24 hr culture.

(I) Flow cytometry of three B cell populations freshly isolated from peripheral blood of healthy donors and then cultured with IL-2, IL-6, IFN- $\alpha$  plus CpG for 96 hr. Three major populations such as CD24<sup>lo</sup>CD27<sup>-</sup>CD38<sup>-</sup> (naive mature; red), CD24<sup>hi</sup>CD27<sup>-</sup>CD38<sup>lo</sup> (naive immature; pink), and CD24<sup>hi</sup>CD27<sup>+</sup>CD38<sup>-</sup> (memory; blue) cells in peripheral blood B cells before culture are gated (left two panels). Percentages of CD27<sup>int</sup>CD38<sup>+</sup> and CD27<sup>hi</sup>CD38<sup>+</sup> cells after culture are shown (right three panels).

(J) ELISA of IL-10 secreted by naive mature, naive immature, and memory B cells isolated from healthy blood donors and cultured with IL-2, IL-6, IFN- $\alpha$  plus CpG for 96 hr.

Data shown are representative of three independent experiments. See also Figure S6.

(B, E, F, H, and J) Data are presented as mean  $\pm$  SD. \*p < 0.05, \*\*p < 0.001 (Student's t test).